Received Date : 19-Aug-2015

Revised Date : 08-Feb-2016

Accepted Date : 20-Feb-2016

Article type : Original Manuscript

Early Mississippian sandy siltstones preserve rare vertebrate fossils in seasonal flooding episodes

Carys E. Bennett[1*], Timothy I. Kearsey[2], Sarah J. Davies[1], David Millward[2], Jennifer A. Clack[3], Timothy R. Smithson[3], John E. A. Marshall[4]

[1]*Department of Geology University of Leicester, Leicester, LE1 7RH*

[2]*British Geological Survey, The Lyell Centre, Research Avenue South, Edinburgh EH14 4AP*

[3]*Department of Zoology, University of Cambridge, Cambridge,* CB2 3EJ

[4]*Ocean and Earth Science, University of Southampton, SO14 3ZH*

* ceb28@le.ac.uk

Associate Editor – Chris Fielding

Short Title – Sandy siltstones from seasonal flooding episodes

ABSTRACT

Flood-generated sandy siltstones are under-recognised deposits that preserve key vertebrate (actinopterygians, rhizodonts, and rarer lungfish, chondrichthyans and tetrapods), invertebrate and plant fossils. Recorded for the first time from the Lower Mississippian Ballagan

This is an Accepted Article that has been peer-reviewed and approved for publication in the *Sedimentology*, but has yet to undergo copy-editing and proof correction. Please cite this article as an "Accepted Article"; doi: 10.1111/sed.12280

Formation of Scotland, more than 140 beds occur throughout a 490 m thick core succession characterised by fluvial sandstones, palaeosols, siltstones, dolostone ‘cementstones’ and gypsum from a coastal–alluvial plain setting. Sandy siltstones are described as a unique taphofacies of the Ballagan Formation. They are matrix-supported siltstones with millimetre-sized siltstone and very fine sandstone lithic clasts. Common bioclasts include plants and megaspores, fish, ostracods, eurypterids and bivalves. Fossils have a high degree of articulation compared with those found in other fossil-bearing deposits such as conglomerate lags at the base of fluvial channel sandstones. Bed thickness and distribution varies throughout the formation, with no stratigraphic trend. The matrix sediment and clasts are sourced from the reworking of floodplain sediments including desiccated surfaces and palaeosols. Secondary pedogenic modification affects 30% of the sandy siltstone beds and most (71%) overlie palaeosols or desiccation cracks. Sandy siltstones are interpreted as cohesive debris flow deposits that originated by the overbank flooding of rivers and due to localised floodplain sediment transport at times of high rainfall; their association with palaeosols and desiccation cracks indicates seasonally wet to dry cycles throughout the Tournaisian. Tetrapod and fish fossils derived from floodplain lakes and land surfaces are concentrated by local erosion and reworking and are preserved by deposition into temporary lakes on the floodplain; their distribution indicates a local origin, with sediment distributed across the floodplain in seasonal rainfall episodes. These deposits are significant new sites that can be explored for the preservation of rare non-marine fossil material and provide unique insights into the evolution of early terrestrial ecosystems.

Keywords: Carboniferous, desiccation, overbank,palaeosol, sandy siltstone, taphofacies, tetrapod, vertebrate

INTRODUCTION

The 25 million years that followed the end of the Devonian (360 Ma) has been regarded as fossil-poor ('Romer's Gap'), attributed in part to the end Devonian mass extinction (Kaiser *et al*., 2015). After the extinction new terrestrial habitats were developed (Davies & Gibling, 2013), fishes reduced in body size (Sallan & Galimberti 2015) and tetrapods started to acquire terrestrial capabilities (Clack, 2002). Now, for the first time anywhere in the world, abundant tetrapod fossils (e.g. Smithson *et al*., 2012) and associated fishes (Smithson *et al*., 2016) have been recovered from this time interval from localities in Scotland, northern England and Nova Scotia (Anderson *et al*., 2015). Why do these particular sedimentary successions preserve such abundant fossil evidence of the early terrestrial ecosystems? What sedimentary processes were acting to concentrate faunal and floral material and, in particular, rare non-marine tetrapod fossils? These successions provide a unique opportunity to enhance and amplify current knowledge of this key time period through the acquisition of new material *within its palaeoenvironmental context*.

Fine-grained mudstone or siltstone overbank facies from floodplain successions preserved in the sedimentary record commonly contain concentrations of vertebrate macrofossils and microfossils (Wilson, 2008; Buck *et al*., 2004). Tetrapod fossils commonly occur in fluvial conglomerate lags and overbank deposits: a review of Euramerican Pennsylvanian tetrapod sites identified swampy pools, oxbow lakes and abandoned fluvial channels filled with organic material as the most common environments where fossils are preserved (Milner, 1987). Late Devonian tetrapods from the East Greenland, Celsius Bjerg Group occur within fluvial sandstones, with associated facies of (overbank) siltstones with thick vertisol sequences (Astin *et al*., 2010). Late Devonian tetrapods from Red Hill, Pennsylvania, USA, were deposited on an alluvial floodplain in an inter-channel deposit consisting of basal lags and overbank deposits (Cressler *et al*., 2010).

The present study is the first to recognise sandy siltstones from the Tournaisian Ballagan Formation as important deposits for the preservation of rare fish and tetrapod fossils. Sandy siltstones are defined here as particulate sedimentary rocks with clasts 1 mm in size (on average), that are supported in a silt-grade matrix. Sandy siltstones are challenging to identify in the field due to their similarity to siltstones, small clast size and friability. Microsites (concentrations of disarticulated vertebrate microfossils where 75% of vertebrate skeletal elements ≤5 cm in size), specifically those which occur in fine-grained sediments (Wilson, 2008; Rogers & Brady, 2010), may be similar deposits, although their detailed sedimentology has not been examined. Other similar deposits are mud aggregates (sand grain sized clay aggregates: Rust & Nanson, 1989) and clay–pebble conglomerates (Buck *et al*., 2004).

The present study records sandy siltstones as a key facies in the Ballagan Formation and provides a detailed sedimentological description and interpretation in the context of the sedimentology of the formation. Macro-features and micro-features are described from core and field sections, with analysis of bed composition, distribution, thickness and structure. The deposits are distinct from other, less common, fossil-bearing sediments in the Ballagan Formation, such as conglomerate lags at the base of metre-scale sandstone bodies and isolated conglomerate beds. The significance of these deposits in terms of sites of fossil preservation and in understanding early Carboniferous climates and environments is discussed.

GEOLOGICAL SETTING

The lower Mississippian (Tournaisian) Ballagan Formation crops out across the Midland Valley of Scotland and in the Scottish Borders, with the entire formation exposed in a 520 m thick vertically-dipping coastal section at Burnmouth, 9 km north of Berwick upon Tweed

(Figure 1), UK. Part of the Inverclyde Group (Figure 2), the Ballagan Formation overlies the Kinnesswood Formation, a succession of fluvial sandstone beds with many rhizocretions (Browne *et al*., 1999; Scott, 1986). The Ballagan Formation encompasses the VI and CM palynozones (Smithson *et al*., 2012; Stephenson *et al*., 2002, 2004a,b; Williams *et al*., 2005). The formation was deposited in a number of north-east/south-west trending active half graben and synclinal basins (such as the Midland Valley of Scotland, Tweed, Solway and Northumberland basins), formed by early Carboniferous extension (Read *et al*., 2002). Sediment may have been sourced from the surrounding highlands such as the Southern Uplands Block (Leeder, 1974) and marine influence is likely to have come from the east (Cope *et al*., 1992).

The Ballagan Formation is characterised by an alternating succession of dolostones (locally known as cementstones), siltstones, palaeosols and sandstones, deposited on a low-lying coastal floodplain (Anderton, 1985; Andrews & Nabi, 1994, 1998; Andrews *et al*., 1991; Scott, 1986; Stephenson *et al*., 2002, 2004a; Turner, 1991). Previous fossil reports from the Ballagan Formation have investigated ostracods (Williams *et al.*, 2006), palynomorphs (Stephenson *et al.*, 2004a), shrimps (Cater *et al.*, 1989), fishes and tetrapods (Clack, 2002, Smithson *et al.*, 2012, 2016). In the Midland Valley of Scotland it was noted that 'macrofauna is sparce' (Williams *et al.* 2005), although abundant plant remains have been recorded (Bateman & Scott, 1990). At Burnmouth the Ballagan Formation is exposed from its contact with the underlying Kinneswood Formation to the base of the overlying Fell Sandstone Formation. The vertically-dipping beds allow the identification of 13 cross-bedded sandstone units, varying in lateral extent and ranging in thickness from 5 to 30 m, most represent fining-upward meandering channels (Anderton, 1985, Greig, 1988). Cementstones, siltstones and palaeosols are the more continuous flat-lying beds that dominate the formation.

Cementstones from the early Carboniferous of the Scottish Borders were deposited in a range of environments from floodplain lakes (Andrews *et al*., 1991) to marginal marine deposits (Belt *et al*., 1967) and are associated with gypsum evaporites (Scott, 1986). The depositional character of the Ballagan Formation alternates between fluvial channels and alluvial plains, lakes and sabkhas, with only rare fossil evidence (orthocones and brachiopods) of marine incursions (Williams *et al*., 2005). Palaeosols, desiccation cracks and brecciated beds are numerous throughout the formation and have previously been associated with cementstones (Andrews *et al.* 1991, Turner, 1991). Sandy siltstone deposits or fossil-rich conglomerates have not previously been identified in field sections or boreholes through the Ballagan Formation and sandy siltstones have most likely been described as grey, black or red siltstones.

In the Tournaisian, Scotland and Northern England were situated 4ºS of the equator (Scotese & McKerrow, 1990), within a tropical climate regime (Peel *et al*., 2007). Tournaisian tree-rings from the Scottish Borders (Falcon-Lang, 1999) and Arundian palaeosols from South Wales (Wright *et al*., 1991) suggest that a monsoonal climate was active. However, the presence of thin evaporites (Scott, 1986) and calcretes (Andrews & Nabi 1998) in the Tweed Basin, halite in the Northumberland Basin (Leeder, 1974) and palaeosols in Southern England (Wright, 1990) give evidence for periodically arid climatic conditions.

MATERIALS AND METHODS

Sandy siltstones were studied from two sites (Figure 1), the coastal field site at Burnmouth and from a 490 m thick fully cored borehole at Norham West Mains Farm (the Norham Core) located about 10 km south-west of Berwick upon Tweed (BGS borehole registered no

NT94NW20). Core recovery of the Ballagan Formation was high although the basal contact with the Kinnesswood Formation was not cored. The core preserves the fidelity of the more friable rocks including the sandy siltstones and palaeosols. Sandy siltstones are better preserved in core, but the exposures enable broader field relationships, such as the lateral extent of sandy siltstones, to be assessed. Field observations and sampling at Burnmouth provide numerous *in situ* tetrapod and fish fossil material from within sandy siltstone beds.

Sedimentary logging of the core and field sections included sampling at approximately metre intervals in both and logging sedimentary units at a centimetre-scale. Sample depths in the core are recorded from the top down, and at Burnmouth are recorded from the base of the Ballagan Formation exposure upward (Appendix 1). Sandy siltstones are described from hand specimens, thin sections, field exposures and from core photographs. The sedimentary features, thickness and fossil content of each sandy siltstone bed recorded are also detailed in Appendix 1. In the field section at Burnmouth, some sandy siltstone beds were identified in rock pools where naturally polished cross-sections of the beds reveal internal structures, but most can only be identified after sample preparation (rock saw or thin section). This process introduces bias attributed to poor exposure caused by weathering, the small clast size and the friability of the beds limiting field identification. Due to this issue, bed distribution, thickness and internal structures are only catalogued from the Norham Core (Appendix 1). Standard-sized, polished thin sections (20 μm thick) were made from 26 Burnmouth and 33 Norham Core sandy siltstone samples. Thin sections were examined on a Leica petrographic microscope (Leica Microsystems, Wetzlar, Germany) and on a Hitachi S-3600N SEM (Hitachi Limited, Tokyo, Japan) at the University of Leicester, using the Back Scattered Electron detector. Fifteen sandy siltstone powder samples were analysed for X-ray

Diffraction (XRD) geochemistry at the University of Leicester using a Bruker D8 Advance (Bruker AXS, Billerica, MA, USA) with DaVinci and DIFFRACplus data analysis software.

Palynological processing and analysis of 12 samples from Burnmouth was undertaken at the University of Southampton employing standard techniques with 5 g of each sample first treated with 30% HCl to remove carbonates followed by decant washing and then 60% HF to complete demineralization. After decant washing to neutral the samples were sieved at 15 µm, placed in a glass beaker with 30% HCl and briefly boiled to dissolve neoformed fluorides. They were then rapidly diluted and resieved with the residue stored in a vial. Slides were permanently mounted in Elvacite 2044. Any megaspores were separated by top sieving at 150 µm and then either bulk mounting in Elvacite or picking through a wet residue under a low power stereoscopic binocular microscope. Fossil material was identified at the University of Cambridge and University of Leicester from surface-sampling on bedding planes and from thin sections. One sample from Burnmouth was analysed by micro-computed tomography (µCT) at the Imaging and Analysis Centre of the Natural History Museum (London, UK) on an X-Tek HMX-ST µCT 225 scanner (Nikon Metrology, Tring, UK). 3142 slices were taken at a resolution of 0.09 mm/voxel, and images were analysed using Mimics software.

FACIES ANALYSIS

The Ballagan Formation consists of ten facies and three facies associations, each of which occur throughout the formation: (i) fluvial facies association; (ii) overbank facies association; and (iii) saline–hypersaline lake facies association (Table 1). In the fluvial facies association the facies are genetically linked, occurring in fining-upward successions of conglomerate lag, cross-bedded sandstone and rippled siltstone (Figure 3, Section 1). The overbank facies association and saline–hypersaline lake facies association alternate on a sub-metre vertical scale, generating packages of siltstones, sandstones, sandy siltstones and palaeosols (Figure 3, section 2). Sandy siltstones are not associated with sandstone channels or sandstones or conglomerates of the overbank facies association. Repeat stacking patterns or cycles within the overbank and saline–hypersaline lake facies associations have not been identified. Rather, facies distribution throughout the sections is fairly heterogeneous. From the base to the top of the formation there is an increase in the number and thickness of palaeosol beds and a decrease in cementstones and laminated grey siltstones.

RESULTS

Sandy siltstone beds occur throughout the Ballagan Formation in the Norham Core (146 beds, Figure 3) and at Burnmouth (71 beds). In the field sandy siltstones are typically grey, have a structureless weathering style (Figure 4A) and contain sporadic visible fossil (plant and bone) fragments (Figure 4B and C). In the core, common features are millimetre-sized clasts in a grey siltstone matrix (Figure 4D and E), soft-sediment deformation at the basal contact (Figure 4D), and internal brecciation (Figure 5C). Sandy siltstone beds occur, on average, every 3.4 m in the core (Figure 3) and comprise 5.6% of the total sediment volume (Table 1). At Burnmouth some units are relatively laterally extensive (over tens of metres), whereas others are lenticular (2 to 5 m). Bed thickness in the core ranges from 0.2 cm to 140 cm (Figs 3 and 6C), with a skewed distribution towards thin beds. There is no correlation between bed thickness and their stratigraphic position (Figure 3).

Composition

Variations in silt grain size and the organic content in the matrix produces a range of bed colours (Figure 5A to D, Appendix 1). In the core the beds are grey (71%), red (19%), black (7%) or green (3%), with a similar colour variation at Burnmouth (Appendix 1). Clasts are either bioclasts or lithic rip-up clasts. Lithoclasts range in size from 6.31 to 0.34 mm (mean 1.4 mm; Figure 6A), with a skewed distribution towards smaller clast sizes; 80% of the measured clasts are within sand grade (2.33 to 0.62 mm). Lithoclasts and bioclasts are sub-angular with a low-sphericity. Clasts are often aligned in thin beds (Figs 4E and 5B). Lithoclasts are predominantly grey or brown siltstone, with minor components of sandstone and black siltstone (Figure 6B). Cementstone clasts are identified only in three beds from the core; two overlie brecciated cementstones, the third has unusually large (5 mm) sub-angular lithic clasts.

X-ray diffraction analysis identified the following minerals: quartz, muscovite, chlorite, interstratified clays, possible kaolinite and feldspars. Minor pyrite, dolomite, calcite and gypsum occur as cements or replacing fossils in certain samples. A high quartz and clay component dominates; the ratio of clay to silt (mostly quartz) is approximately 3:2, although this varies between and within beds. During borehole coring, wall erosion frequently occurred where metre-thick sandy siltstones are present. Wireline geophysical logging revealed a high neutron porosity that signifies a high clay-bound water content, which corresponds to the expansion and disintegration upon wetting of hand specimens.

Fossil content

Bioclasts are mostly composed of plant fragments and fish debris (Figure 6E). The proportion of bioclasts to lithoclasts is on average 3:7, but is highly variable between each bed. Bioclast size ranges from sub-millimetre (megaspore fragments) to several centimetres (bone fragments). The average size of bioclast fragments approximately correlates with the size of lithoclasts within the same bed, excluding larger bone fragments. Plants comprise fragments of leaf and stem, lycopsid root, charcoal, megaspores and wood. Invertebrates include ostracods (*Shemonaella* and *Paraparchites)*, bivalves (*Modiolus* and *Naiadites*) and eurypterid cuticle. Very rare invertebrates are shrimps, *Spirorbis* sp. *Serpula* sp., orthocones and scolecodonts (Figure 6E). Vertebrates include actinopterygians, rhizodonts, and rarer lungfish, chondrichthyans and tetrapods. Twelve samples analysed for palynomorphs recovered spores, megaspores, charcoal and arthropod cuticle fragments. In addition, one sample contains two scolecodonts, but this bed also contains rip-up clasts of the underlying grey siltstone at its base, so the origin of the scolecodonts is uncertain.

Sandy siltstones contain a similar fauna to that identified in other clastic lithologies in the formation, but the fossil abundance, especially of plants and vertebrates, is higher. The taphonomy of the fossil deposits has not been examined in detail, but some observations can be made in this regard. Fossil articulation is significantly better compared with other lithologies, for example articulated rhizodont lepidotrichia are observed (Figure 4C). In comparison, all fossil material is disarticulated in conglomerate lag deposits, fossils are rarely preserved in palaeosols and grey siltstones have a lower fossil abundance. Articulated ostracod carapaces and bivalves occur in sandy siltstones, even within the basal crack-fills. Fossils examined with a binocular microscope do not appear to have any abrasion or breakage, although further detailed investigation is needed to confirm this.

Sedimentary structures

Internal structures vary according to bed thickness (Figure 6D), with laminae more common in thinner units (<2 cm thick). Rip-up clasts at the base of units are irregular to angular in shape and associated with soft sediment deformation. Most beds are ungraded, but some thicker units (greater than 1 m thick) are normally graded, with larger clasts at the base and a top that grades into grey siltstone (Figure 7). The tops of sandy siltstone units are usually bioturbated (Figure 8B, Section 2), rooted or brecciated. Some sandy siltstone successions intercalate with thin (sub-centimetre thick) siltstone beds and, in these examples, clasts are generally aligned parallel to bedding. Internal brecciation has been identified in 15 beds and desiccation cracks within two beds in the core. Internal brecciation is distinct from desiccation cracks because the fracture boundaries are irregular (Figure 4C) and partially gradational (for example, Figure 8A, Section 1). Internal brecciation is most common within thicker beds (mean 36.5 cm thickness), pedogenically modified beds (50% of those with brecciation) and beds with pedogenic slickensides. Variations in sedimentary structure are controlled by clast size, the relative position (height within a bed) and the degree of post-depositional modification (summarised in Figure 7). In thicker sandy siltstones (*ca* 1 m thick), the clast size can be normally graded, whereas thin deposits show limited variations in clast size.

Pedogenic and diagenetic modification

Secondary pedogenic modification of sandy siltstones affects 30% of beds in the core and stacked successions of palaeosols and sandy siltstones are common. Red and yellow mottles, red or gley (greenish grey) coloured matrix, within-bed colour gradations, *in situ* roots and slickensides are identified as pedogenic features (Figs 4F and 5F). Brown siltstone clasts are commonly mottled and are similar petrologically to palaeosols. Pedogenically modified sandy siltstones have a lower fossil content. Sandy siltstones commonly grade into palaeosols, with an increase in the extent of pedogenesis towards the top of the bed (Figs 4F and 7A, Section 2); 47% of beds in the core that overlie sandy siltstones are pedogenically modified or brecciated. Pedogenic slickensides are pervasive, even in apparently un-modified beds, which may be a result of stacked sandy siltstone/palaeosol successions. Rarely, sandy siltstone beds are partially or completely cemented by dolomite, altering the sediment to a cementstone (dolostone) lithology.

Associated Facies

Most sandy siltstones recorded in the core (71%) overlie sediments that exhibit brecciation, pedogenic modification or desiccation cracks; these comprise palaeosols (51%), cementstones (11%) and sandstones (9%). The rest overlie unmodified sandstone, siltstone and cementstone; 23% of the brecciated surfaces contain cracks infilled with sandy siltstone, and the clasts within these infills are typically disordered (Figs 4D and 5A). The cracks range in depth from 4 to 60 cm (mean 18 cm), narrow downward from the top of the bed to their tip and have an irregular polygonal structure on the bed surface that identifies them as desiccation cracks (c.f. Plummer & Gostin, 1981). Cracks are generally associated with pedogenic features but can also occur in unmodified lithologies. There is no correlation between crack depth and thickness of the overlying sandy siltstone unit. Lithologies overlying sandy siltstone beds include siltstone, sandstone and cementstone with no predominant pattern, although the pedogenic alteration of these overlying beds is common.

Comparison with other tetrapod-bearing units

Tetrapod material has also been recovered from thin, lenticular conglomerate beds and conglomerate lags. Eight discontinuous conglomerates occur in the Burnmouth section and two in the core; they have a lateral extent of only a few metres, are not related to larger sandstone bodies and occur within the overbank facies association. Key features include a fine sandstone matrix, sub-angular clasts, poorly sorted, with 0.5 to 1.0 cm sized clasts (Table 1). Each bed is different in terms of clast composition, structure and thickness. One bed from

Burnmouth contains centimetre-sized cementstone clasts with internal lamination similar to that seen in the Pease Bay conglomerate (Andrews *et al.*, 1991). Fossils present in this facies include plant and wood fragments, ostracods, rhizodont and actinopterygian scales and fin rays (lepidotrichia).

Ten conglomerate lags occur at the base of metre-thick cross-bedded sandstones at Burnmouth and 13 occur in the core. The units are normally graded, poorly sorted and comprise sub-angular pebble-sized clasts of cementstone, sandstone and siltstone within a fine to medium sandstone matrix (Table 1). Larger fossil elements, such as Gyracanthid spines and tetrapod and rhizodont bones, are commonly present whereas plant fragments, ostracods, bivalves and actinopterygian fragments are rarer. The main distinction from sandy siltstones is the larger clast size in conglomerates, the presence of cementstone clasts, and their fossil composition.

INTERPRETATION

Sandy siltstones are interpreted as unconfined flow deposits that transported out of channel sediment across an alluvial floodplain; they occur within the overbank facies association and are not genetically related to fluvial deposits. Unconfined flows may develop directly from the overland flow produced by local precipitation, or may develop out of flow in channels by processes that release that flow from confinement (North & Davidson, 2012). This is schematically illustrated in Figure 9, where sandy silts are deposited after flooding events, over an alluvial plain that is vegetated, marshy or desiccated. Unconfined alluvial flow deposits have been described previously as sheetflow, sheetfloods or flash floods, although a review of their sedimentology reveals these terms are unreliable and unsuitable for use (North & Davidson, 2012). The sedimentology of the deposit, possible formation mechanisms, sedimentological context and climate are all considered here when interpreting these heterogeneous sediments.

The depositional mechanism is interpreted as cohesive debris flows (mudflows), based on the classification of Lowe (1982), with deposits typically defined as ungraded, matrix-supported, with clasts fully suspended in the matrix. The main evidence for this interpretation is: (i) matrix-supported fabrics; (ii) the commonly structureless nature of thicker beds; (iii) sub-angular to angular clasts; (iv) soft sediment deformation; (v) the absence of bioturbation within sandy siltstone beds; and (vi) the general absence of desiccation cracks within beds. Although predominantly structureless, the presence of lamination within centimetre-thick beds, weak bedding in thicker units and graded bedding indicates that changes in the flow velocity or sediment concentration occurred. For example, a drop in sediment concentration within the flow could lead to changes in bedforms from structureless, nongraded units to parallel lamination (Postma, 1986). The sporadic presence of aligned clasts is interpreted to indicate changes in flow velocity or direction. This is to be expected when taking into account potential surface topographic variations of the floodplain.

A local sediment source is likely because the clast composition is the same as that of the underlying lithologies. The matrix and clasts are derived from the reworking of floodplain sediments, with 23% of clasts (brown siltstones) originating from palaeosols. Primary evidence for low-velocity of deposition is the small average clast size, especially compared with that of the conglomerate lags (an order of magnitude larger). Secondary evidence is the rare occurrence of cementstone clasts (which by contrast commonly occur within conglomerates), despite the fact that 11% of sandy siltstone beds overlie brecciated cementstone surfaces. This indicates that most of the floods either did not have enough energy to rip up this dense dolostone or to transport the brecciated fragments. Additionally, the articulated nature of many fossils, including fish, ostracod and bivalves, suggests a local origin with minimum transport, although the distance of transport is hard to determine based on fossil-content alone. Flow rheology can also be influenced by factors such as its cohesive strength, thickness, density and viscosity (Postma, 1986), it is difficult to estimate accurate flow velocities based on these observations.

Desiccation cracks are common within pedogenically modified coastal–alluvial plain sediments, such as those from the Visean of Fife (Fielding & Frank, 2015). The rare presence of desiccation cracks within two sandy siltstone units indicates the stacking of multiple sandy siltstone beds produced in more than one flooding event. However, internal brecciation textures are much more common than desiccation cracks within sandy siltstone units. They are similar to soil crusts and vesicular surface horizons seen in modern saline-sodic wetland soils (Joeckel & Clement, 2005). These features form by daily to seasonal cycles of wetting and drying, microbial activity or salt development. The internal brecciation features are commonly associated with pedogenesis and may indicate: (i) waterlogged conditions, with temporary vegetation growth in some cases; or (ii) changes in the water table resulting in internal brecciation due to sediment drying.

An important facies association of sandy siltstone beds is their occurrence on top of, and infilling desiccation cracks. The process of crack-fill is likely to have been passive, meaning that the flows did not have enough energy to create or widen the cracks. This is based on the following evidence: (i) the presence of articulated fossil material within the cracks; (ii) the thickness of the overlying sandy siltstone bed does not correspond to the depth of the cracks;

and (iii) there is no clast alignment within the cracks. In the Cretaceous Hasandong Formation of Korea, vertic palaeosols form in floodplain deposits, and have a variety of desiccation cracks: deep desiccation cracks with unbridged sediment infill formed close to the active fluvial channel, while cracks infilled with calcite mineral precipitate or rhizocretions formed in more distal positions to the active fluvial channel (Paik & Lee, 1998). In addition, Paik & Lee (1998) identified cracks with a vertically stratified infill of sandstone and mudstone as indicating seasonal wetting and drying stages. The absence of these types of complex infills in the present study indicates that cracks were not exposed for a long period, and that infill was instantaneous.

Stacked successions of sandy siltstone and palaeosols containing desiccation cracks are interpreted to represent periods of relatively dry depositional conditions (Figure 8A). These are distinguished from intervals without palaeosols and desiccation cracks, and are interpreted as deposited in a more waterlogged environment, sometimes directly into floodplain lakes (Figure 8B). Successions of stacked sandy siltstones and palaeosols are more common and are the result of seasonally wet conditions. The random, but common occurrence of sandy siltstones throughout the Ballagan Formation and variable bed thickness indicates that deposition was controlled by processes on the floodplain, such as rainfall within the catchment, the extent and type of vegetation and variations in basin topography. Continuous and steady basin subsidence would be required to generate the accommodation needed for these alluvial deposits. There is no evidence of base-level drop and incised valleys in the formation, or syn-sedimentary faults indicative of tectonic shifts.

The rarity of thick sandy siltstone beds (>20 cm) indicates that most of the depositional flooding events were of low magnitude. This interpretation is consistent with the observation that flood magnitude is inversely correlated with flood frequency (e.g. Knighton, 1998), producing common thin and rare thick deposits. Seasonal to monsoonal short-term changes in the climate are proposed as the mechanism for these frequent, local flooding episodes. A tropical palaeoclimate with seasonal rainfall and monsoonal influence has been proposed for the Tournaisian of the British Isles, based on fossil tree growth ring patterns of gymnosperms, including specimens from Burnmouth (Falcon-Lang, 1999). The presence of evaporites within the Norham Core (Table 1), Burnmouth (Scott, 1986), the Midland Valley of Scotland (Belt *et al.*, 1967) and siltstone pseudomorphs after halite in the Northumberland Basin (Leeder, 1974) indicate that the region experienced times of periodic aridity and/or marine influence. The formation does not contain any distinctive marine bands, such as those in the overlying Strathclyde Group (Fielding & Frank, 2015). Despite the geographic proximity of shallow-seas (Cope *et al.*, 1992), the sparse marine to marginal marine faunal occurrences indicate that sea-level changes were minimal, with perhaps only short-lived marine incursions. While gypsum associated with dolomite can form in coastal evaporitic lakes or lagoons (for example in the Coorong Region, Australia: Wacey *et al.*, 2007), they can also form periodically in coastal floodplain wetlands subject to evaporation and occasional marine influence (for example in the Tigris-Euphrates marshes during the Holocene: Aqrawi 1995). The lack of a marine fauna within the Ballagan Formation indicates that periods of climate aridity and evaporation may have increased the salinity of coastal water bodies to an extent where they became hypersaline, although a marine groundwater source may also have been involved. In Southern Britain, evidence from palaeosols and palaeokarsts during the Tournaisian indicate a seasonally semi-arid environment at this time (Wright, 1990). Despite this, palaeosols and sandy siltstones comprise 20.6% of the sediment thickness in the Norham

Core, compared with only 3.0% thickness of evaporites (Table 1), demonstrating that although arid conditions occurred, they were not prevalent, and seasonally wet, possibly monsoonal, conditions were dominant. A comparable analogue is the Late Devonian Red Hill site of the Catskill Formation, with a similar vertebrate and plant assemblage deposited in floodplain settings with vertisols, interpreted as a seasonal wetland environment (Cressler, 2006, Cressler *et al*., 2010).

The conglomerate lag deposits at the base of fluvial bodies represent the transport and deposition of sediments and fossil material as bedload. Reviews of Upper Cretaceous Judith River Formation (USA) microsites interpret the source of vertebrate material in conglomerate lag deposits was probably from re-working microfossil deposits in ponds and lakes (Rogers & Brady, 2010). The clast composition of conglomerate lags from the Ballagan Formation indicates that they are sourced from reworked floodplain deposits including cementstone clasts from saline–hypersaline lakes. In a study on the stratigraphic correlation potential of vertebrate-bearing fluvial conglomerate lag deposits, Rogers & Kidwell (2000), demonstrated that these were deposited in topographic depressions, with material derived from the surrounding facies (laterally or underlying the lags), and that the lag deposits do not necessarily correlate with times of sea-level fall or sequence stratigraphic discontinuity surfaces.

Lenticular conglomerate beds of the Ballagan Formation within the overbank facies association have clasts derived from reworked floodplain sediments, lakes (cementstones) and palaeosols. These have similar characteristics to thin lenses of sand–matrix conglomerates recorded from the Old Red Sandstone of Wales (Marriott & Wright, 1996) and the Pease Bay conglomerate (Andrews et al., 1991). Compared with the conglomerate at the Pease Bay succession (Andrews et al., 1991) the clast and matrix size of the Burnmouth and Norham Core lenticular conglomerates are smaller, although the fossil content is similar. A similar overbank flooding formation mechanism could have formed both deposits. Conglomerates with a high clast density could be related to those formed by hyperconcentrated density flows, which are often caused by catastrophic flooding events (Benvenuti & Martini 2002).

DISCUSSION

Dryland river systems have a significant overbank component (Tooth, 2000). Modern dryland rivers in Australia provide a good modern analogue for the common dry/wet alternations seen in the palaeosol/sandy siltstone associations. In these systems pedogenic mud aggregates overlie desiccation cracks (Rust & Nanson, 1989, Wakelin-King & Webb, 2007a,b). Examples in the geological record occur in the Lower Devonian Lower Old Red Sandstone of South Wales (Ékes 1993, Marriott & Wright, 2004), in the Upper Triassic Lunde Formation of the northern North Sea (Müller *et al*., 2004) and in Upper Cretaceous playa-lake and sheetflood deposits of the Jindong Formation, Korea (Paik & Kim, 2006). In the Jindong Formation the frequent alternation of palaeosols containing desiccation cracks, evaporites and thin sheetflood deposits (Paik & Kim, 2006) is similar to that of the palaeosol–sandy siltstone facies association of the Ballagan Formation. In these modern and ancient examples, mud aggregates are derived from vertisols and are deposited across the floodplain in sheetflows. Deposition took place first from suspension and then as bedload, producing bedding, clay layers and ripples; their preservation in the rock record comprises a largely structureless clay-rich unit with poorly expressed bedding and a horizontal fabric. In these arid settings red-coloured alluvial sediments (vertisols), red clay units (flood deposits) and sandstones with gravel (channel deposits) are typical. Silt-sized to 4 mm mud aggregate clasts are recorded in modern and geological deposits, with most studies classifying them as sand-sized (Marriott & Wright, 2004, Müller *et al*., 2004, Rust & Nanson, 1989 and Wakelin-King & Webb, 2007b). A flume-tank study of mud aggregate deposits from dryland river settings highlighted that most clasts that were formed were very small (0.13 mm), but tension wetting to model high intensity rainfall, generated clasts up to 0.7 mm in size (Maroulis & Nanson, 1996).

The main differences between mud aggregates and sandy siltstones are: sandy siltstone clasts are typically larger; lithoclasts are heterogeneous rather than monomict mud aggregates; abundant plant, vertebrate and invertebrate fossils are present in sandy siltstones; and the internal structures and associated depositional mechanisms are different. In addition, the largely grey colour of the sandy siltstones and their dominant clasts indicates that wetland conditions were more common than dryland. Seasonal wetlands exist in the areas surrounding rivers in modern dryland settings, as in southern Africa today (Tooth & McCarthy, 2007). The presence of desiccation cracks below sandy siltstones and charcoal within them indicates that the climate was seasonally dry, with occasional fires on the floodplain, then wet with overbank and overland flooding episodes. Mud aggregates from a non-vegetated floodplain have similar locally derived clasts and desiccation crack-fill textures as the sandy siltstones (Fralick & Zaniewski, 2012) but lack the plant material. There is a greater similarity with the Upper Triassic 'reworked mud aggregates' of Müller *et al*. (2004), which have packages with a sharp to erosive base, varied clast composition, including re-worked pedogenic carbonate nodules, and matrix composition, rounded/smooth clasts and millimetre size clasts. Permian/Triassic claystone breccias (Retallack, 2005) have some similarities to sandy siltstones, in that they contain clasts derived from palaeosols and wood and plant material, in a fine-grained matrix. These breccia deposits are interpreted as the products of significant soil erosion following the end Permian extinction event. Sandy siltstones have a much lower concentration of sepic pedoliths and are likely to be formed by simple flooding of a desiccated floodplain environment, rather than the result of complete landscape erosion.

The heterogeneous clast composition within sandy siltstones and high plant content indicates a varied alluvial plain environment that was vegetated (Figure 9). The common occurrence of sandy siltstone beds may indicate that plant rooting systems were unable to be firmly established due to the high frequency of flooding events, or that vegetation on the floodplain was sparse. The sediment source area was poorly vegetated in the Mississippian compared with the transfer and deposition zones (Corenblit *et al*., 2015). Upland areas are likely to have been poorly vegetated compared with the Pennsylvanian (Falcon-Lang & Bashforth, 2004). The extinction of many plant groups such as *Archaeopteris* trees at the Hangenberg event affected the terrestrial landscape, with the main radiation of trees not occurring until the mid–late Tournaisian (Decombeix *et al*., 2011). This broadly coincides with changes in river morphology in the Mississippian, with the advent of anastomosing river systems linked to the stabilisation of floodplains and river banks by trees (Davies & Gibling 2011, 2013). The Ballagan Formation can be contrasted with the Early Pennsylvanian Joggins Formation of Nova Scotia, where there is significant *in situ* vegetation, rather than transported, indicating that the lycopsid, calamitalean and cordaitalean vegetation in alluvial environments had a stabilising effect on the river systems and overbank deposits (Ielpi *et al*., 2015). However, the identification of *in situ* vegetation can be a product of the availability of well-exposed bedding planes in field sections. Further investigation into the plant communities present within sandy siltstones is needed in order to discuss trends in the vegetated floodplain through the Tournaisian at this site.

The sedimentology and most of the flora and fauna identified indicate a mixture of terrestrial (plants and arthropods) to freshwater (bivalves, fish and ostracods) conditions. However, some species are salinity tolerant, so variations in salinity must be considered. Lycopsid roots can occur in terrestrial to deep bodies of standing water (Philips & DiMichele, 1992), and occur in freshwater to saline wetland or salt marsh environments (Rygel *et al*., 2006, Raymond *et al*., 2010). Lycopsid-dominated coals recorded from the Pennsylvanian of Iowa are thought to represent freshwater mangroves that grew in an extremely wet climate (Raymond *et al*., 2010). *Modiolus* bivalves are thought to be indicators of freshwater, but other invertebrates such as *Naiadites* bivalves and *Shemonaella* and *Paraparchites* ostracod species are brackish to euryhaline (Bennett *et al*., 2012, Williams *et al*., 2005, 2006). Actinopterygians, rhizodonts and lungfish in the Ballagan Formation are thought to be euryhaline, or brackish to freshwater tolerant (Carpenter *et al*., 2014). The eurypterid, acanthodian and tetrapod groups from this time period have unknown salinity tolerances. However, the assemblage of sarcopterygians, dipnoans, chondrichthyans, acanthodians and tetrapods is comparable to that of other freshwater–brackish deposits in the Mississippian of the USA (Garcia *et al.*, 2006) and UK (Carpenter *et al.*, 2014). The assemblage is also similar to some Late Devonian sites (apart from the absence of placoderms) that are interpreted as early freshwater habitats (Cressler *et al.* 2010*,* Denayer *et al*. 2016).

Spirorbis, Serpula, shrimps, orthocones and scolecodonts are rare (Figure 6E), but represent more marine components: *Spirorbis* has been recorded from a range of palaeoenvironments and considered to be a euryhaline organism (Zatoń *et al*., 2012). However, its reclassification as a microconchid with phoronid affinities (Taylor & Vinn, 2006) has led to a re-evaluation of the published record of Palaeozoic–Mesozoic specimens, and the conclusion that it is marine in origin (Gierlowski-Kordesch & Cassle, 2015). The salinity tolerance of

Carboniferous *Serpula* is less well-known, with records from a wide range of salinity (Burchette & Riding, 1977). Shrimps are known from marginal marine to brackish environments in the Carboniferous (Briggs & Clarkson, 1989). Three sandy siltstone beds contain marine fauna: one scolecodont (marine worm jaw) and two orthocone fragments, which are most likely to have originated from rip-up clasts derived from underlying marine sediments. Mud aggregate deposits have been recorded from shallow-marine ramp settings (Plint *et al*., 2012). These differ from sandy siltstones described in this study by having smaller and sparser clasts that are predominantly composed of clay-sized grains, a lower proportion of plant fragments, and an association with distinctive shallow marine sedimentary structures, such as hummocky cross-stratification.

The fossils within the sandy siltstones are likely to originate from a number of different environments. The mixture of terrestrial and aquatic animals and abundance of plant material indicates that the floods incorporated material from land surfaces and water bodies. Palaeosols inhabited by arthropods and tetrapods may have existed within a floodplain landscape containing fresh to brackish water bodies inhabited by actinopterygians, rhizodonts, ostracods and bivalves. Overall the fauna indicates brackish water salinity (Williams *et al*., 2006), which indicates the proximity of shallow seaways during the Tournaisian (Cope *et al*., 1992). However, waters that were originally fresh may have become more saline over time due to evaporation. During flooding episodes the sediments and fossils within these fresh or brackish water bodies would then be ripped-up and transported across the vegetated floodplain or deposited into existing lakes. Sandstone clasts may have originated from rivers, streams or crevasse-splay deposits, although silt grained clasts are most common, indicating a local floodplain origin. The articulated nature of ostracods and bivalves indicates fossil transport while alive, which may also have been the case for the terrestrial arthropods and tetrapods, although further taphonomic investigation is needed to validate this hypothesis.

Overbank facies commonly comprise a greater volume than fluvial facies and the flooding of river systems is much more common than previously thought (Syvitski *et al.*, 2012). Overbank deposits can be important sites of preservation of tetrapod fossils, for example at the Late Devonian Red Hill site (Cressler *et al.*, 2010). Although the aggregated thickness of sandy siltstone beds in the Norham Core represents only 6% of the total sediment thickness, they record flooding events that provide a greater insight into overbank processes; they form a distinctive taphofacies that preserve rare fossils from Romer's Gap, due to the nature of their deposition as a cohesive flow. Sandy siltstone deposits containing tetrapods have not previously been described, but some uses of the terms microsites, mud aggregates, siltstones or conglomerates could document the same lithology. The Late Devonian tetrapod-bearing Britta Dal Formation sedimentary rocks of the Celsius Bjerg Group, Greenland, comprise mostly vertisols deposited as mud aggregates in seasonal flooding events (Astin *et al.*, 2010), with an environment analogous to the arid Cooper Creek in Australia. Further study is required to ascertain whether some of the siltstone vertisols may be modified sandy siltstones, although the environment as a whole is much more arid. The Late Devonian Red Hill tetrapod site of Pennsylvania, USA, contains four fossil-bearing taphofacies; microfossil, basal lag, channel margin and standing water. The standing water taphofacies is described as "*green-grey siltstones with abundant plant material & an occasional occurrence of arthropod & vertebrate remains*" (Cressler et al. 2010) and may be similar to the sandy siltstones.

The fossil-rich Foulden beds of the Ballagan Formation exposed in the Scottish Borders show many similarities to sandy siltstone units (Anderton, 1985). The Foulden Fish Bed is 30 cm thick and is composed of millimetre to centimetre thick beds of fining-up very fine sandstone and siltstone. These beds have sharp bases, sporadic lamination or cross-lamination and contain abundant plant and fossil fragments and mud clasts. The average size of the clasts is not recorded and the deposits are not identified as sandy siltstones, but the succession records a sequence of short-lived flooding events into a lake. One major difference compared with the Burnmouth and Norham Core sandy siltstones is the absence of pedogenic horizons. The coal-bearing siltstone successions of the Pennsylvanian Joggins Formation of Nova Scotia may also include sandy siltstones in the green-grey siltstones of the poorly-drained floodplain facies assemblage (Davies & Gibling, 2003). The Lower Pennsylvanian Buffalo Wallow Formation of Hancock County, Kentucky, contains a comparable vertebrate fauna of tetrapods, dipnoans, rhizodonts, actinopterygians, acanthodians and chondrichthyans within abandoned channel and oxbow facies (Garcia *et al.*, 2006, Greb *et al.*, 2015). Although sandy siltstones are not identified, tetrapod remains are also found within rooted siltstone palaeosol horizons, which could be analogous to the original environment of the Ballagan Formation tetrapods.

Examples of deposits that contain similarly high concentrations of vertebrate microfossils are the Upper Cretaceous Conor's Microsite, a siltstone-rich crevasse splay deposit with clay clasts (Wilson, 2008); and fine-grained microsite deposits from the Upper Cretaceous Judith River Formation with bivalves, interpreted as autochthonous pond/lake deposits (Rogers & Brady, 2010). Clay-pebble conglomerates with 2 mm to 8 cm sized clasts composed of sand and granule sized mud aggregates from the Cretaceous–Tertiary of the Nanxiong Basin, Southern China, are interpreted as distal sheetfloods (Buck *et al*. 2004). These deposits may be similar to the discontinuous conglomerates of the Ballagan Formation. Tetrapods from conglomerate lag deposits within sandstones have been recovered from the Tournaisian Horton Bluff Formation of Blue Beach, Nova Scotia (Anderson *et al*., 2015). The sedimentology of this formation is similar to the Ballagan Formation, including black-grey shales, although sandy siltstones have not been recorded so far from this formation (Martel, 1990, Tibert & Scott, 1999). Isolated tetrapod bones are commonly recorded from conglomerate lags in the Carboniferous, such as at Grand Étang, Nova Scotia (Holmes *et al*., 1995), and sites in central New Mexico (Harris *et al*., 2004). Sites with tetrapods preserved in fluvial systems probably have an overbank facies component and in these cases it might be worth investigating the presence of a potential sandy siltstone-type taphofacies.

Sandy siltstones are key sites for vertebrate preservation due to two factors: (i) the concentration of fossils by predominantly overbank flooding erosion and transportation processes; and (ii) rapid deposition inhibiting disruption by bioturbation. The high clay content of the sandy siltstones is important in preserving fossil specimens; equally important is that most are not pedogenically modified. The recognition of these fossil specimens throughout a 500 m thick, early Carboniferous, alluvial-coastal plain succession indicates they are an important depositional mechanism on these seasonally-wet floodplains and may provide key locations for preservation of flora and fauna to understand the palaeocology of these depositional settings. Other siltstone-grade overbank deposits are worth re-evaluating in terms of their potential to be sandy siltstones and thus non-marine fossil-rich deposits.

CONCLUSIONS

- This study is the first to recognise the repeated occurrence of sandy siltstones and their association with the highest concentration of vertebrates (including rare tetrapod and fish material), invertebrates (bivalves, ostracods and arthropods) and flora in the Lower Mississippian Ballagan Formation. The recognition and interpretation of this taphofacies reveals the frequent transport of fine-grained sediment across seasonally wet floodplains and identifies these units as key sites for fossil preservation.
- Sandy siltstones are matrix-supported siltstones with clasts of siltstone or very fine sandstone that are on average 1 mm in size. The clasts and fossils were sourced from local floodplain sediments, including palaeosols, and from desiccated lakes and marsh environments. Sandy siltstones occur throughout the Ballagan Formation. The 490 m thick Norham Core yields 146 sandy siltstone beds. Bed thickness can range up to 140 cm, although most beds are less than 10 cm thick.
- Most of the sandy siltstone beds are deposited directly overlying palaeosol beds or desiccation cracks. The facies association, bed thickness distribution, internal structure and composition of the sandy siltstones indicate deposition in flooding events that were relatively localised. Flooding events probably occurred due to seasonal precipitation and the sediments were deposited as cohesive debris flows into temporary lakes on the floodplain. A seasonal climate with dry to wet alternations is proposed for the Tournaisian of Scotland and the Scottish Borders.
- The deposits are distinguished from discontinuous conglomerates and conglomerate lags at the base of fluvial sandstone bodies, which also contain fish and tetrapod material, by their composition, their unique facies association with palaeosols and their fidelity of fossil preservation.

- Sandy siltstones are friable, typically poorly exposed in field outcrops and their small clast size means that they may be overlooked or categorised as siltstones or as monomict mud aggregates. A re-examination of these types of overbank deposits in the rock record could potentially reveal many more rare non-marine fossils.

ACKNOWLEDGEMENTS

This study is a contribution to the TW:eed Project (Tetrapod World: early evolution and diversification), a major research programme investigating the rebuilding of Carboniferous ecosystems following a mass extinction at the end of the Devonian (Smithson *et al.*, 2012). This study was funded by NERC Consortium Grant '*The Mid-Palaeozoic biotic crisis: setting the trajectory of tetrapod evolution*' led by Dr Jenny Clack (University Museum of Zoology, Cambridge) and involving the Universities of Cambridge (NE/J022713/1), Leicester (NE/J020729/1), Southampton (NE/J021091/1), the British Geological Survey (NE/J021067/1) and the National Museum of Scotland. The following TW:eed Project volunteers are thanked for their assistance with fossil identification from sandy siltstone beds: Catherine Caseman, Rachel Curtis, Levi Curry, Rowan DeJardin, Daniel Downs, Hattie Dulson, Deborah Fish, Susan Hammond, Catherine Langford, Graham Liddiard, Jessica Mason, James Mawson, Kirsty Summers and Thomas Worthington. Daniel Sykes at the Natural History Museum, London, is thanked for technical assistance with micro-CT scanning and Keturah Smithson at the University of Cambridge for micro-CT image processing. DM and TIK publish by permission of the Executive Director, British Geological Survey (NERC). We thank Scottish Natural Heritage for their permission to allow us to take samples for study at the SSSI site of Burnmouth. Julian Andrews, Colin North and one anonymous referee are thanked for their constructive comments in reviewing this manuscript.

REFERENCES

Anderson, J.S., Smithson, T., Mansky, C.F., Meyer, T. and **Clack, J.** (2015) A Diverse Tetrapod Fauna at the Base of 'Romer's Gap'. *PLoS ONE*, **10**, 1-27, doi:10.1371/journal.pone.0125446.

Anderton, R. (1985) Sedimentology of the Dinantian of Foulden, Berwickshire, Scotland. *Trans. Roy. Soc. Edinb. Earth Sci.*, **76**, 7-12.

Andrews, J.E. and **Nabi, G.** (1994) Lithostratigraphy of the Dinantian Inverclyde and Strathclyde Groups, Cockburnspath Outlier, East Lothian–North Berwickshire. *Scot. J. Geol.,* **30,** 105-119.

Andrews, J.E. and **Nabi, G.** (1998) Palaeoclimatic significance of calcretes in the Dinantian of the Cockburnspath Outlier (East Lothian-North Berwickshire). *Scot. J. Geol.,* **34**, 153-164.

Andrews, J.E., Turner, M.S., Nabi, G. and **Spiro, B.** (1991) The anatomy of an early Dinantian terraced floodplain: palaeo-environment and early diagenesis. *Sedimentology,* **38**, 271-287.

Aqrawi, A.A.M. (1995) Brackish-water and evaporitic Ca-Mg carbonates in the Holocene lacustrine/deltaic deposits of southern Mesopotamia. *J. Geol. Soc. Lond.*, **152**, 259-268.

Astin, T.R., Marshall, J.E.A., Blom, H. and **Berry, C.M.** (2010) The sedimentary environment of the Late Devonian East Greenland tetrapods. In: *The terrestrialisation process: Modelling complex interactions at the Biosphere-Geosphere Interface* (Eds M. Vecoli, G. Clément and B. Meyer-Berthaud). *Geol. Soc. Spec. Publ.*, **339**, 93-109.

Bateman, R.M. and **Scott, A.C.** (1990) A reappraisal of the Dinantian floras at Oxroad Bay, East Lothian, Scotland. 2. Volcanicity, palaeoenvironments and palaeoecology. *Trans. Roy. Soc. Edinb. Earth Sci* , **81**, 161-194.

Belt, E.S., Freshney, E.C. and **Read, W.A.** (1967) Sedimentology of Carboniferous cementstone facies, British Isles and Eastern Canada. *J. Geol.*, **75**, 711-721.

Bennett, C. E., Siveter, D. J., Davies, S. J., Williams, M., Wilkinson, I. P., Browne, M. and **Miller, C. G.** (2012) Ostracods from freshwater and brackish environments of the Carboniferous of the Midland Valley of Scotland: the early colonisation of terrestrial water bodies. *Geol. Mag.*, **149**, 366-396.

Benvenuti, M. and **Martini, I.P.** (2002) Analysis of terrestrial hyperconcentrated flows and their deposits. *Flood and Megaflood Processes and Deposits: Recent and Ancient Examples, Int. Assoc. Sedimentol. Spec. Publ.*, **32**, 167-193.

Briggs, D.E.G. and **Clarkson, E.N.K.** (1989) Environmental controls on the taphonomy and distribution of Carboniferous malacostracan crustaceans. *Trans. Roy. Soc. Edinb. Earth Sci.*, **80**, 293-301.

Browne, M.A.E., Dean, M.T., Hall, I.H.S., McAdam, A.D., Monro, S.K. and **Chisholm, J.I.** (1999) A lithostratigraphical framework for the Carboniferous rocks of the Midland Valley of Scotland. *British Geological Survey Research Report RR/99/07.*

Buck, B.J., Hanson, A.D., Hengst, R.A. and **Shu-sheng, H.** (2004) "Tertiary Dinosaurs" in the Nanxiong Basin, Southern China, are reworked from the Cretaceous. *J. Geol.*, **112**, 111-118.

Burchette, T.P. and **Riding, R.** (1977) Attached vermiform gastropods in Carboniferous marginal marine stromatolites and biostromes. *Lethaia* **10**, 17-28.

Carpenter, D.K., Falcon-Lang, H.J., Benton, M.J. and **Henderson, E.** (2014) Carboniferous (Tournaisian) fish assemblages from the Isle of Bute, Scotland: systematics and palaeoecology. *Palaeontology*, **57**, 1215-1240.

Cater, J.M.L., Briggs, D.E.G. and **Clarkson, E.N.K.** (1989) Shrimp-bearing sedimentary successions in the Lower Carboniferous (Dinantian) Cementstone and Oil Shale groups of northern Britain. *Trans. Roy. Soc. Edinb. Earth Sci.*, **80**, 5-15.

Clack, J.A. (2002) An early tetrapod from ‘Romer's Gap’. *Nature*, **418**, 72-76.

Cope, J.C.W., Guion, P.D., Sevastopulo, G. D, and **Swan, A.R.H.** (1992) Carboniferous. Pp 67-86 in: Cope, J. C. W., J. K. Ingham, and Rawson P F (editors). Atlas of palaeogeography and lithofacies. Geological Society of London Memoir No 13.

Corenblit, D., Davies, N.S., Steiger, J., Gibling, M.R. and **Bornette, G.** (2015) Considering river structure and stability in the light of evolution: feedbacks between riparian vegetation and hydrogeomorphology. *Earth Surf. Proc. Land.* **40**, 189-207.

Cressler, W.L. (2006) Plant paleoecology of the Late Devonian Red Hill locality, north-central Pennsylvania, an Archaeopteris-dominated wetland plant community and early tetrapod site. *Geol. Soc. Spec. Publ.*, **399**, 79-102.

Cressler, W.L., Daeschler, E.B, Slingerland, R. and **Peterson, D.A.** (2010) Terrestrialization in the Late Devonian: a palaeoecological overview of the Red Hill site, Pennsylvania, USA. In: *The terrestrialisation process: Modelling complex interactions at the Biosphere-Geosphere Interface* (Eds M. Vecoli, G. Clément and B. Meyer-Berthaud). *Geol. Soc. Spec. Publ.*, **339**, 111-128.

Davies, S.J. and **Gibling, M.R.** (2003) Architecture of coastal and alluvial deposits in an extensional basin: the Carboniferous Joggins Formation of eastern Canada. *Sedimentology*, **50**, 415-439.

Davies, N.S. and **Gibling, M.R.** (2011). Evolution of fixed-channel alluvial plains in response to Carboniferous vegetation. *Nature Geoscience*, **4**, 629-633.

Davies, N.S. and **Gibling, M.R.** (2013). The sedimentary record of Carboniferous rivers: Continuing influence of land plant evolution on alluvial processes and Palaeozoic ecosystems. *Earth-Sci. Rev.*, **120**, 40-79.

Decombeix, A.L., Meyer-Berthaud, B. and **Galtier, J.** (2011) Transitional changes in arborescent lignophytes at the Devonian–Carboniferous boundary. *J. Geol. Soc.*, **168**, 547-557.

Ékes, C. (1993) Bedload-transported pedogenic mud aggregates in the Lower Old Red Sandstone in southwest Wales. *J. Geol. Soc. Lond.*, **150**, 469-471.

Falcon-Lang, H.J. (1999) The early Carboniferous (Courceyan-Arundian) monsoonal climate of the British Isles: evidence from growth rings in fossil woods. *Geol. Mag.*, **136**, 177-187.

Falcon-Lang, H.J. and **Bashforth, A.R.** (2004) Pennsylvanian uplands were forested by giant cordaitalean trees. *Geology*, **32**, 417-420.

Fielding, C.R. and **Frank, T.D.** (2015) Onset of the glacioeustatic signal recording late Palaeozoic Gondwanan ice growth: New data from palaeotropical East Fife, Scotland. *Palaeogeogr. Palaeoclimatol. Palaeoecol.*, **426**, 121-138.

Fralick, P. and **Zaniewski, K.** (2012) Sedimentology of a wet, pre-vegetation floodplain assemblage, *Sedimentology*, **59**, 1030-1049.

Garcia, W.J., Storrs, G.W. and **Greb, S.F.** (2006) The Hancock County tetrapod locality: A new Mississippian (Chesterian) wetlands fauna from western Kentucky (USA). *Geol. Soc. Spec. Pap.*, **399**, 155-167.

Gierlowski-Kordesch, E.H. and **Cassle, C.F.** (2015) The '*Spirorbis*' Problem Revisited: Sedimentology and Biology of Microconchids in Marine-Nonmarine Transitions. *Earth-Sci. Rev.*, **148**, 209-227.

Greb, S.F., Storrs, G.W., Garcia, W.J. and **Eble, C.F.** (2015) Late Mississippian vertebrate palaeoecology and taphonomy, Buffalo Wallow Formation, western Kentucky, USA. *Lethaia*. DOI: 10.1111/let.12138.

Greig, D.C. (1988) Geology of the Eyemouth district. *Memoir of the British Geological Survey*, Sheet 34.

Harris, S.K., Lucas, S.G., Berman, D.S. and **Henrici, A.C.** (2004) Vertebrate fossil assemblage from the Upper Pennsylvanian Red tanks member of the Bursum Formation, Lucero uplift, central New Mexico. In: Lucas, S.G., Zeigler, K.E. (eds). Carboniferous-Permian transition. *New Mexico Museum of Natural History and Science Bulletin*, **25**, 267-283.

Holmes, R., Godfrey, S. and **Baird, D.** (1995) Tetrapod remains from the late Mississippian Pomquet Formation near Grand Étang, Nova Scotia. *Can. J. Earth Sci.*, **32**, 913-921.

Ielpi, A., Gibling, M.R., Bashforth, A.R. and **Dennar, C.I.** (2015) Impact of Vegetation On Early Pennsylvanian Fluvial Channels: Insight From the Joggins Formation of Atlantic Canada. *J. Sed. Res.*, **85**, 999-1018.

Joeckel, R. and **Clement, B.A.** (2005) Soils, surficial geology, and geomicrobiology of saline-sodic wetlands, North Platte River Valley, Nebraska, USA. *Catena* **61**, 63-101.

Kaiser, S.I., Aretz, M. and **Becker, R.T.** (2015) The global Hangenberg Crisis (Devonian–Carboniferous transition): review of a first-order mass extinction. *Geol. Soc., London, Spec. Publ*, **423**, http://doi.org/10.1144/SP423.9.

Knighton, D. (1998) Fluvial Forms and Processes: a New Perspective, 2nd Edition. Arnold, London. 383 pp.**Leeder, M.R.** (1974) Lower Border Group (Tournaisian) fluvio-deltaic sedimentation and palaeogeography of the Northumberland Basin. *Proc. Yorks. Geol. Soc.,* **40**, 129-180.

Lowe, D.R. (1982) Sediment gravity flows: II Depositional models with special reference to the deposits of high-density turbidity currents. *J. Sed. Res.*, **52**, 279-297.

Maroulis, J.C. and **Nanson, G.C.** (1996) Bedload transport of aggregated muddy alluvium from Cooper Creek, central Australia: a flume study. *Sedimentology*, **43**, 771–790.

Marriott, S.B. and **Wright, V.P.** (1996) Sediment recycling on Siluro-Devonian floodplains. *J. Geol. Soc. London*, **153**, 661-664.

Marriott, S.B. and **Wright, V.P.** (2004) Mudrock deposition in an ancient dryland system: Moor Cliffs Formation, Lower Old Red Sandstone, southwest Wales, UK. *Geol. J.*, **39**, 277-298.

Martel, A.T. (1990) Stratigraphy, Fluviolacustrine Sedimentology and Cyclicity of the Late Devonian/Early Carboniferous Horton Bluff Formation, Nova Scotia, Canada. Unpublished Ph.D. Thesis, Dalhousie University, Halifax, 297 p.

Milner, A.R. (1987) The Westphalian tetrapod fauna; some aspects of its geography and ecology. *J. Geol. Soc. London*, **144**, 495-506.

Müller, R., Nystuen, J.P. and **Wright, V.P.** (2004) Pedogenic Mud Aggregates and Paleosol Development in Ancient Dryland River Systems: Criteria for Interpreting Alluvial Mudrock Origin and Floodplain Dynamics. *J. Sed. Res.*, **74**, 537-551.

North, C.P. and **Davidson, S.K.** (2012) Unconfined alluvial flow processes: Recognition and interpretation of their deposits, and the significance for palaeogeographic reconstruction. *Earth-Sci. Rev.*, **111**, 199-223.

Paik, I.S. and **Lee, Y.I.** (1998) Desiccation cracks in vertic palaeosols of the Cretaceous Hasandong formation, Korea: genesis and palaeoenvironmental implications. *Sed. Geol.*, **119**, 161-179.

Paik, I.S. and **Kim, H.J.** (2006) Playa lake and sheetflood deposits of the Upper Cretaceous Jindong Formation, Korea: Occurrences and palaeoenvironments. *Sed. Geol.*, **187**, 83-103.

Peel, M.C., Finlayson, B.L. and **McMahon, T.A.** (2007) Updated world map of the Köppen-Geiger climate classification. *Hydrology and Earth System Sciences Discussions, European Geosciences Union*, **11**, 1633-1644.

Phillips, T.L. and **DiMichele, W.A.** (1992) Comparative ecology and life-history biology of arborescent lycopsids in Late Carboniferous swamps of Euramerica. *Ann. Miss. Bot. Gar.*, 560-588.

Plint, A.G., Macquaker, J.H.S. and **Varban, B.L.** (2012) Bedload transport of mud across a wide, storm-influenced ramp: Cenomanian-Turonian Kaskapau Formation, Western Canada Foreland Basin. *J. Sed. Res.*, **82**, 801-822.

Plummer, P.S. and **Gostin, V.A.** (1981) Shrinkage cracks: desiccation or synaeresis. *J. Sed. Petrol.*, **51**, 1147–1156.**Postma, G.** (1986) Classification for sediment gravity-flow deposits based on flow conditions during sedimentation. *Geology*, **14**, 291-294.

Raymond, A. Lambert, L., Costanza, S. Slone, E.J. and **Cutlip, P.C.** (2010) Cordaiteans in paleotropical wetlands: An ecological re-evaluation. *Int. J. Coal. Geol.*, **83**, 248-265.

Read, W.A., Browne, M.A.E., Stephenson, D. and **Upton, B.G.J.** (2002) Carboniferous. In: Trewin, N.H. (Ed.), The Geology of Scotland, 4th edition. The Geological Society London, pp. 251–299.

Retallack, G.J. (2005) Earliest Triassic claystone breccias and soil-erosion crisis. *J. Sed. Res.*, **75**, 679-695.

Rogers, R.R. and **Brady, M.E.** (2010) Origins of microfossil bonebeds: insights from the Upper Cretaceous Judith River Formation of north-central Montana. *Paleobiology*, **36**, 80-112.

Rogers, R.R. and **Kidwell, S.M.** (2000) Associations of vertebrate skeletal concentrations and discontinuity surfaces in terrestrial and shallow marine records: a test in the Cretaceous of Montana. *J. Geol.*, **108**, 131-154.

Rust, B.R. and **Nanson, G.C.** (1989) Bedload transport of mud as pedogenic aggregates in modern and ancient rivers. *Sedimentology*, **36**, 291-306.

Rygel, M.C., Calder, J.H., Gibling, M.R., Gingras, M.K. and **Melrose, C.S.A.** (2006) Tournaisian forested wetlands in the Horton Group of Atlantic Canada. *Geol. Soc. Am. Spec. Publ.,* **399**, 103-126.

Sallan, L. and **Galimberti, A.K.** (2015) Body-size reduction in vertebrates following the end-Devonian mass extinction. *Science*, **350**, 812-815.

Scotese, C.R. and **McKerrow, W.S.** (1990) Revised world maps and introduction. *Geol. Soc. London Mem.* **12**, 1-21.

Scott, W.B. (1986) Nodular carbonates in the Lower Carboniferous, Cementstone Group of the Tweed Embayment, Berwickshire: evidence for a former sulphate evaporite facies. *Scot. J. Geol.*, **22**, 325-345.

Smithson, T.R., Wood, S.P., Marshall, J.A.E. and **Clack, J.A.** (2012) Earliest Carboniferous tetrapod and arthropod faunas from Scotland populate Romer's Gap. *PNAS*, **109**, 4532-4537.

Smithson, T.R., Richards, K.R. and **Clack, J.A.**, (2016) Lungfish diversity in Romer's Gap: reaction to the end-Devonian extinction. *Palaeontology*, **59**, 29-44.

Stephenson, M.H., Williams, M., Monaghan, A.A., Arkley, S. and **Smith, R.A.** (2002) Biostratigraphy and palaeoenvironments of the Ballagan Formation (Lower Carboniferous) in Ayrshire. *Scot. J. Geol.*, **38**, 93-111.

Stephenson, M.H., Williams, M., Leng, M.J. and **Monaghan, A.A.** (2004a) Aquatic plant microfossils of probable non-vascular origin from the Ballagan Formation (Lower Carboniferous), Midland Valley, Scotland. *Proc. Yorks. Geol. Soc.*, **55**, 145-158.

Stephenson, M.H., Williams, M., Monaghan, A.A., Arkley, S., Smith, R.A., Dean, M., Browne, M.A.E. and **Leng, M.** (2004b) Palynomorph and ostracod biostratigraphy of the Ballagan Formation, Midland Valley of Scotland, and elucidation of intra-Dinantian unconformities. *Proc. Yorks. Geol. Soc.,* **55**, 131-143.

Syvitski, J.P., Overeem, I., Brakenridge, G.R. and **Hannon, M.** (2012) Floods, floodplains, delta plains—a satellite imaging approach. *Sed. Geol.*, **267**, 1-14.

Taylor, P.D. and **Vinn, O.** (2006) Convergent morphology in small spiral worm tubes ("*Spirorbis*") and its palaeoenvironmental implications. *J. Geol. Soc. London*, **163**, 225-228.

Tibert, N.E. and **Scott, D.B.** (1999) Ostracodes and agglutinated foraminifera as indicators of palaeoenvironmental change in an Early Carboniferous brackish bay, Atlantic Canada. *PALAIOS*, **14**, 246-260.

Tooth, S. (2000) Process, form and change in dryland rivers: a review of recent research. *Earth-Sci. Rev.*, **51**, 67-107.

Tooth, S. and **McCarthy, T.S.** (2007) Wetlands in drylands: geomorphological and sedimentological characteristics, with emphasis on examples from southern Africa. *Progress in Phys. Geog.*, **31***,* 3-41.

Turner, M.S. (1991) Geochemistry and diagenesis of basal Carboniferous dolostones from southern Scotland. *Unpublished Ph. D. thesis, University of East Anglia.*

Wacey, D., Wright, D.T. and **Boyce, A.J.** (2007). A stable isotope study of microbial dolomite formation in the Coorong Region, South Australia. *Chem. Geol.,* **244**, 155-174

Wakelin-King, G.A. and **Webb, J.A.** (2007a) Upper-Flow-Regime Mud Floodplains, Lower-Flow-Regime Sand Channels: Sediment Transport and Deposition in a Drylands Mud-Aggregate River. *J. Sed. Res.*, **77**, 702-712.

Wakelin-King, G.A. and **Webb, J.A.** (2007b) Threshold-dominated fluvial styles in an arid-zone mud-aggregate river: The uplands of Fowlers Creek, Australia. *Geomorphology*, **85**, 114-127.

Waters, C.N. (2011) A revised correlation of Carboniferous rocks in the British Isles. *Geol. Soc. Lond. Spec. Rep.*, **26**, pp190.

Williams, M., Stephenson, M. H., Wilkinson, I. P., Leng, M. L. and **Miller, C. G.** (2005) Early Carboniferous (Late Tournaisian-Early Viséan) ostracods from the Ballagan Formation, central Scotland, UK. *J. Micropal.*, **24**, 77-94.

Williams, M., Leng, M. L., Stephenson, M. H., Andrews, J. E., Wilkinson, I. P., Siveter, D. J., Horne, D. J. and **Vannier, J. M. C.** (2006) Evidence that Early Carboniferous ostracods colonised coastal flood plain brackish water environments. *Palaeogeogr. Palaeoclimatol. Palaeoecol.,* **230**, 299-318.

Wilson, L.E. (2008) Comparative taphonomy and paleoecological reconstruction of two microvertebrate accumulations from the Late Cretaceous Hell Creek Formation (Maastrichtian), Eastern Montana. *PALAIOS*, **23**, 289–297.

Wright, V.P. (1990) Equatorial aridity and climatic oscillations during the early Carboniferous, southern Britain. *J. Geol. Soc. London*, **147**, 359-363.

Wright, V., Vanstone, S. and **Robinson, D.** (1991) Ferrolysis in Arundian alluvial palaeosols: evidence of a shift in the early Carboniferous monsoonal system. *J. Geol. Soc.* **148**, 9-12.

Zatoń, M., Vinn, O. and **Tomescu, A.M.F.** (2012) Invasion of freshwater and variable marginal marine habitats by microconchid tubeworms – an evolutionary perspective. *Geobios*, **45**, 603-610.

FIGURE CAPTIONS

Figure 1. Location map Scotland and Northern England, illustrating the location of the Burnmouth field section and the site of the Norham borehole (National Grid Reference 391589, 648135). Maps modified from Smithson *et al.*, 2012.

Figure 2. Lithostratigraphy of the Ballagan Formation, Early Carboniferous, adapted from Waters (2011) and Smithson *et al.* (2012). The grey unit represents an erosional surface and overlying hiatus.

Figure 3. Sandy siltstone distribution in the Norham core. The stratigraphic height and thickness of each sandy siltstone bed is plotted, in comparison to palaeosols, which show a fairly good correspondence. The frequency curve (number of sandy siltstone beds per 10 m) indicates a random bed distribution throughout the formation. Sandstone beds of the fluvial facies association (Table 1) are highlighted in yellow on the sedimentary log. There is a

greater frequency of sandy siltstone beds in between units of thick fluvial sandstones. Desiccation cracks are common throughout the section, often occurring below sandy siltstone beds. Section 1 illustrates an example of the Fluvial and Saline-Hypersaline Lake facies associations. The Fluvial facies association is characterised by fining-upward cross-bedded sandstones or thinner rippled sandstone beds. The Saline-Hypersaline Lake facies association consists of interbedded or stacked cementstones and grey siltstones. Section 2 illustrates key features of the Overbank facies association, characterised by grey siltstones, sandy siltstones, sandstones and palaeosols. Bed lithology varies on a sub-metre scale, with thin cementstones representing short-lived intervals of the Saline-Hypersaline Lake facies association. Part of the section with extensive pedogenic alteration (209 to 213 m) is shown in more detail in Figure 8.

Figure 4. Key sandy siltstone features. (A) Field photograph showing a black sandy siltstone (M; arrow points to top of bed) overlain by grey siltstones, Burnmouth, at 374 m. (B) Close-up image of a sandy siltstone bed with a bone fragment (arrow), Burnmouth, at 340.5 m. (C) Micro-CT scan of the same bed as in (B), illustrating abundant fossils (mostly rhizodonts) concentrated on certain horizons. The large clast is very unusual and most clasts are millimetre in size. (D) Thick sandy siltstone, with crack-fill and soft sediment deformation (ssd) at the base, then aligned clasts (c) suspended in silt, Norham Core, at 157 m. (E) A thin laminated sandy siltstone bed with small clasts (c, arrow), Norham Core, at 226 m. The bed overlies a bioturbated sandstone and incorporates a sandstone burrow at its base. (F) Pedogenic sandy siltstone with internal brecciation, Norham Core, at 281 m. Scale details: (A) and (B) camera lens cap, 5 cm diameter; (C) to (F) scale bars, 2 cm.

Figure 5. Sandy siltstone features in thin section. (A) Sandy siltstone infilling cracks in an underlying palaeosol, SSK 38473, Norham Core at 262.28 m. (B) A typical centre of a sandy siltstone bed, BURN/13/06/S_CLIFFS/7c, Burnmouth, at 334.85 m. (C) Internal

fracturing/brecciation in the centre of a sandy siltstone bed, SSK 38158, Norham Core, at 381.91 m. (D) Sandy siltstone with siltstone-sized clasts, BURN/12/10/S_CLIFFS/82, Burnmouth, at 340.8 m. (E) SEM image of the area identified in image (D), illustrating quartz clasts (q) and bone fragments (b) within a clay-rich matrix. (F) Pedogenically modified sandy siltstone, with an increase in alteration towards the top, SSK 39026b, Norham Core, at 123.17 m. Scale bars: 250 µm (A) to (D) and (F); and 50 µm (E).

Figure 6. Sandy siltstone clast size, clast composition, thickness, structure and fossil composition. (A) Clast size range for each clast lithology from a measured set of 100 clasts. The minimum, maximum and mean (black square) size is shown; the mean clast size is 1.4 mm (for all lithologies). (B) Clast composition percentage plot from the same samples measured for clast size. For (A) and (B) 10 clasts were measured in a thin section of 10 representative samples from Burnmouth and the Norham Core (Appendix 1), bioclasts were excluded from measurements. (C) Thickness frequency plot with bin groupings of 10 cm (Norham Core). (D) Sandy siltstone bed structure occurrence plots for thick (>2 cm) and thin (< 2 cm) beds (Norham Core). Percentage plots illustrate the most dominant structural feature present in each bed. More of the thin sandy siltstones are laminated compared to thicker units. (E) Fossil composition data of sandy siltstone beds. The percentage of beds containing each fossil type is shown, non-fossil bearing beds are not included. For example, in the Norham Core plants are present in 67% of the sandy siltstone beds that contain fossils. Fossils are present in 57 out of 146 sandy siltstone beds in the Norham Core and 66 out of 71 beds in Burnmouth; further details can be found in Appendix 1. A greater number of fossils were recovered from field samples (Appendix 1) due to the larger rock mass available for study. Fossil name caption: Fish other refers to lungfish, chondrichthyans and tetrapods. Eurypterids are the most common arthropod fossil, but rare shrimps and myriapods also occur. Indet. = indeterminate.

Figure 7. Schematic illustration of the variability of sandy siltstone structures viewed in thin section. The range of structures present are related to clast size, position within thick beds (relative height from base), or type of alteration is illustrated. Images are drawn using thin section samples as a reference guide; each image has a width of 20 mm.

Figure 8. End-member sandy siltstone depositional settings in the Norham Core. (A) Deposition onto dry floodplain. The sandy siltstone beds were deposited during river overbank flooding events or due to localised high rainfall floods, between relatively arid periods when desiccated sediments were common. Section 1: Two brecciated palaeosol beds with sandy siltstone infill of cracks in the upper unit. Section 2: A brecciated sandy siltstone bed overlain by a palaeosol. (B) Deposition onto wet floodplain. The thick sandy siltstone was deposited onto wet overbank sand deposits, and a fresh to brackish water lake was established. Section 1: Central part of a thick sandy siltstone, with bedding at the base and internal brecciation at the top. Section 2: Top of a bedded sandy siltstone, comprising an extensively brecciated lighter grey unit, with soft sediment deformation, overlain by a black, normally graded sandy siltstone. The upper 3 cm of the sandy siltstone is laminated and contains ostracods, plant fragments, *Spirorbis* sp. and *Naiadites* sp. The key for the sedimentary logs is given in Figure 3.

Figure 9. Schematic diagram of the palaeoenvironment during sandy siltstone formation. Prior to flooding events meandering fluvial systems, marshes, palaeosol formation on floodplains, desiccating pools and lakes occur. During flooding sandy siltstone deposition (ss) occurs in overbank deposits and in shallow meteoric-fed lakes. Vegetation is not shown.

Table 1. Facies Analysis of the Ballagan Formation. The facies volume (%) is based on thickness measurements from the 490 m long Norham Core, which contains a more complete

(well-preserved) record of fine-grained sediments than the field section. Facies descriptions are based on both Norham Core and Burnmouth field section observations.

Early Carboniferous sandy siltstones preserve rare vertebrate fossils in seasonal flooding episodes

Supplementary Papers

Appendix 1. Key features of sandy siltstone beds.

Norham Core

Height (m)	Thickness (cm)	Colour	Lithological Description	Fossils
501.1	35	grey	laminated, soft sed def, brecciated	ostracods, *Modiolus* sp., plant frags, megaspores? bivalves
500	2	grey	weakly laminated	actinopt bone; scorpion cuticle, plants, ostracods
489.25	28.5	grey	disrupted structures, pedogenic slickensides	
486.65	10	grey	fractured in core box	
483.9	22.5	grey	structureless, sparce gypsum nodules	
481.95	25	grey	laminated	plant frags, abundant *Modiolus* sp. *Naiadites* sp., ostracods, actinopt frags
479.42	18	grey	structureless	
478.15	17.5	grey	structureless	*Modiolus*, bivalves, biot top
470.8	5	grey	structureless	
464.35	18.5	grey	structureless	
452.1	101.5	black	clasts of black clay/silt, weak bedding	pyritised plant frags, lycopsid-like roots, ostracods
442.75	2.5	grey	clasts of mud, aligned, sand-rich matrix	plant frags
441.98	20	grey	bedded, clasts of silt and plant frags	plant frags
440.2	15	grey	coarsens up, no bedding, brecciated	plant frags (abundant)
438.55	110	grey	structureless, fractured in core box	
428.8	12	grey	mud clasts, pedogenic, yellow nodules	actinopt scale
428.52	8	grey	structureless	actinopt frags, biot top, bivalve mould (?*Modiolus* sp.)
427.35	14	grey	sandy base, fines up, mud clasts, bedded	rooted
426.85	57.5	grey	clasts of black silt/clay and cementstone, bedded, pedogenic	abundant plant frags, roots? biot?
426.4	16.5	grey	pyrite nodules and grey silt lenses	plant frags
419.03	2	grey	clasts of grey silt	plant frag?
395.25	25	grey	fines-up, rip-ups of underlying silt at base	

393.05	5	grey	structureless, clasts of red and grey silt	
391.75	3	red	pedogenic, rooted	
387.1	7.5	grey	black and grey silt clasts, structureless	biot base
384.15	43	grey	structureless	
383.65	5	grey	soft sed def	
381.9	34	black	green mottles, soft sed def to structureless	plant frags, ostracods
381.3	57	red/grey	weak bedding/laminae at base, silt clasts, pedogenic top, yellow mottles	plant frags, rooted
379.58	2	grey	structureless	
378.8	11	grey	structureless	
373.95	2.5	grey	laminated	plant frags
373.45	80	grey	weakly bedded, fractured, mostly structureless, rip-ups of sand at base	rooted, plant frags, actinopt bone, scorpion cuticle, ostracods
372	74	grey	pedogenic, soft sed def, some large clasts	rooted
370.52	17.5	grey		
351.28	7.5	grey	laminated	
351.15	2	grey	weakly laminated	
349.89	8	grey	soft sed def structures of green silt	actinopt scale
348.3	22	red	weakly bedded, pedogenic	
346.55	3	grey	pedogenic, red mottles	
344.75	74	red	clay-rich base, weakly bedded, pedogenic,	rooted
342.05	25	grey	soft sed def, brecciated top	rooted top
336.6	2	grey	weakly laminated	
334.47	6	grey	pedogenic, red mottled	
327.22	9.5	grey	pedogenic, yellow/red mottled, black laminae	
326.62	7	grey	pedogenic, laminated, red mottles	
326.5	5	grey	structureless	
317.9	11	grey	structureless, pedogenic, red mottles	rooted?
301.37	19	grey	structureless	
281.25	70	grey	pedogenic, slickensides, brecciated	plant frags, fish frags
276.32	6.5	grey	laminated, brecciated top, sandy matrix	ostracods?, scorpion cuticle, actinopt frags, bivalves
263.98	1	black	laminated	organic-rich
263.85	1	grey	sand-rich, clasts of silt and plant frags	plant frags
261.78	63	grey	red mottled, pedogenic, laminated top	plant frags
260.9	8	grey	structureless	
260.7	25	grey	structureless, brecciated top	biot, plant and fish frags
259.32	22	red	fines up, pedogenic, top, brecciated	
243.2	33	grey	clasts of black and red silt, cementstone band in centre, weakly bedded, some clast alignment	plant frags
241.55	30	grey	bedded, very organic-rich at base	plant frags
239.65	8	grey	structureless	

228.98	4.5	grey	structureless	fish frags
228.57	2	grey	soft sed def, rip-ups of cementstone	
226.67	1	grey	structureless	
226.62	3	grey/white	sand-rich, aligned clasts, coarsens-up	plant? Frags
226.02	3	grey	loaded base, aligned clasts	biot
225.33	4	grey	rip-ups at base of underlying silt	
224.19	4.5	grey	laminated top	
224.1	4	grey	laminated top	
223.25	22	red	pedogenic, red and yellow mottles, cracks	
218.75	118	grey/black	laminated top, brecciated centre	plant and fish frags, *Naiadites* sp., *Spirorbis* sp, ostracods
217.54	5	grey/green	laminated, pedogenic, black clasts	
211.1	5	grey	black silt clasts, grades into a grey silt	bivalves, *Modiolus latus*
210.1	20	grey/red	aligned clasts, grey base, pedogenic top	
209.55	26	grey	bedded/soft sed def, brecciated top, pedogenic	
209.25	3	grey	laminated, organic-rich black top	
209.2	0.5	grey	laminated	
209.18	0.5	grey	laminated	
208.93	1	grey	aligned clasts, soft sed def	
208.85	1	grey	structureless	
206.9	13	grey	extensively brecciated, desiccation cracks	
206.05	2	red	pedogenic, laminated	
206	4	red	pedogenic, laminated	
205.81	3	red	pedogenic, laminated	
202.98	140	grey	fines up, red and yellow mottles, cracks	rooted at base?
200.92	2	grey	top is loaded into by sands	
199.78	0.2	red	laminated, pedogenic	
196.7	18	grey	pedogenic, brecciated, sot sed def	
196	20	grey	pedogenic, brecciated	
195	24	red	pedogenic, brecciated	fish spine
193.2	32	grey	soft sed def at base, rip-ups of underlying grey silt, fines into laminated grey silt	plant frags
192.35	28	grey	fractured in core box	
184.84	3	grey/red	bedded, grey base, red middle, grey top	
179.58	18	grey/red	bedded,, red colour, with two grey beds within, aligned clasts, pedogenic	
178.7	13	grey/black	with flow structures	plant frags
178.6	0.2	black	laminated	
177.17	1.5	grey	structureless, abundant grey silt clasts	
162.5	87	grey	peodgenic, yellow mottles, soft sed def/rip-ups, highly brecciated top	rooted?, plant frags
156.25	75	grey	pedogenic, yellow mottles, some iron-oxide spots, rip-ups of underlying silt at base, brecciated centre, and extensively brecciated at top	biot?, fish scale, ?bone, plant frags, ostracods
142.07	10	black	organic-rich silt, with pyrite nodules, lamination and mm thick coalified seams	rhizodont, actinopt, plants, charcoal, ostracods
139.05	32	grey	bedded, brecciated in centre	
135.82	41	grey	bedded, soft sed def, stacked sequence	plant frags, bone?
135.3	7.5	grey/white	soft sed def, carbonate cemented	

134.33	15	grey	structureless to weakly bedded	
130.75	75	grey/red	pedogenic, grey base, red top	
129.6	31	red	pedogenic	
123.17	5	black/red	bedded, pedogenic	plant frags
122.75	0.5	grey/white	silt rip-ups	
122.37	4	grey	structureless	
121.8	65	green/grey	pedogenic, extensively brecciated base, soft sed def top with black sandy siltstone	rooted
119.3	73	red	bedded, mottled, pedogenic	small roots, plant frags
115.39	10	grey	rip-up clasts of underlying silt at base, fines up, top laminated with thin coalified seams	biot, plant frags, coalified seams, orthocone frag
113.75	8	grey	structureless	
113.25	61	grey	laminated base, pedogenic, brecciated top, bedded	
106.22	40	red	grey mottles	
85.95	10	grey	aligned clasts at base, brecciated top	
85.55	2	black	mottled, pedogenic	
83.82	12	grey	structureless	plant and fish frags
74.9	34	red	yellow mottles	rooted?
70.3	33	grey	pedogenic, rip-up clasts of underlying red silt at base with iron-oxide nodules	
70	1	grey/white	mud clasts in a sandy matrix	
67.95	17	grey	soft sed def, with palaeosol rip-ups at base, weakly bedded	rooted
67.76	1	grey	structureless	large plant frags
67.17	8	grey	brecciated	
55.75	20	grey	yellow mottled	
54.95	32	black	highly fractured	
50.97	13	grey	soft sed def, rip-ups at base	
48.8	0.2	red	laminated	
48.76	0.2	red	laminated	
48.7	0.2	red	laminated	
48.42	0.2	grey		
47.4	5	grey	red mottled	
43.85	0.2	grey/green	laminated, red mottles at base	
43.77	0.2	grey/green	laminated, red mottles at base	
41.48	2	grey	laminated, soft sed def	
40.23	17	grey	fractured core in box	
39	8	grey	red mottles	
38.35	1	red	bedded, fines up	
37.64	1.5	red	pedogenic	
37.51	2	red	pedogenic	
37.18	4	grey	laminated	plant frags
31.45	17	grey	bedded, red/grey mottled throughout, yellow mottles, irregular bed boundaries with red silt	
30.37	6.5	grey	base fills desiccation cracks, structureless	large plant frags
30.22	3	grey	red mottled	
28.57	3	red	grades into red silt	
27.94	3	red		

Burnmouth field section

33.8	grey		frags of rhizodont, lungfish, actinopt, gyracanthus, tetrapod, *Ageleodus*, plant, charcoal
45.3	grey	no laminae	shelly fossil frags, bivalves?
45.55	grey	soft sed def, rip-ups, slickensides, bedded	roots, plant frags
46.85	grey	laminated, black mud clasts, slickensides	biot or rooted
50	grey	laminated, soft sed def, rip-ups	rooted, actinopt, cuticle, *Paraparchites* sp. ostracods, lungfish frags
55.45	grey	soft sed def, mud and silt clasts	fish scales, ostracods, scorpion cuticle
76.17	grey	pedogenic, brecciated, no internal laminae	charcoal, plant frags, sparce roots
76.32	grey	pedogenic, v f sand/silt matrix, brecciated	scale frags, ostracods (*Glyptolichvinella* and others)
76.55	grey	pedogenic, sand clasts, soft sed def	plant frags, thick roots, charcoal, *Shemonalla* sp. ostracods
77.85	grey	soft sed def, silt-rich	plant frags, rooted, ostracods, lungfish bone, rhizodont frag
78.63	grey	brecciated?	ostracods (poor), *Paraparchites* sp., *Shemonaella* sp.?
89.95	grey	silt-rich at base	
90.65	grey	laminated, flow structures	actinopt scales
91.25	grey	soft sed def	
93.55	grey	base fills cracks, brecciated, soft sed def	rooted?, pyritised ostracods, plant frag, cuticle frag
107.75	grey	mud clasts	plant and fish scale frags
108.03	grey	mud clasts	
132.85	grey	mudstone rip-up clasts, water-escape structures	ostracods
179.2	grey	mottled colour, slickensides, soft sed def	fish scales
180.9	black	laminated, slickensides, soft sed def	abundant plant frags, wood frag, cuticle, fish scales, *Paraparchites* sp., *Shemonaella* sp. ostracods, megaspores
182.35	grey	laminated, black mud clasts	biot
183.15	grey		biot, cuticle, plant frags, actinopt frags
204	grey	laminated, mud clasts, soft sed def	plant frags, actinopt frags, bivalve indet, megaspores?
211.75	grey	laminated, granule size silt rip-up clasts	2 scolecodonts
241.65	grey	grey and red mud rip-up clasts	sparce fish scales
242.55	grey	grey silt rip-up clasts	
256.35	grey	silt and mud clasts, disrupted laminae	fish scales
274.25	grey	bedded, clasts of silt	plant, bone?, fish scales
280.85	grey/red	yellow/red mottled	extensively rooted, plant frags, fish scales, bone frag, bivalve?, ostracods (poor)

287.1	grey	mud rip-up clasts, slickensides	plant and fish scale frags
288.15	red/grey	mottled, matrix-supported, rip-up clasts	rooted?
300	grey	disrupted laminae, clay and sand clasts	plant frag, bone frag
334.85	grey	large clasts, soft sed def, slickensides	plant frags
334.95	grey		plant, bone and scale frags, actinopt scale and tooth, sparce ostracods
337	grey	deformation textures, very small clasts	plant frags
338.35	grey	black clasts	plant frags
338.5	grey	black mudstone rip-ups	plant, actinopt and cuticle frags
340.45	grey	crack fill at base, very fine grain size and clasts	ostracods (common), plant, fish (indet.) and lungfish frags
340.55	grey	laminated, large clasts	frags of rhizodont, actinopt, gyracanthus, tetrapod, *Ageleodus*, chondrichthyans, plants, ostracods
340.65	black		charcoal, frags of plants, actinopts, rhizodonts, eurypterids
340.85	black	laminated	plant frags, actinopt scale, rhizodont scales, cuticle
341	grey/black	laminated	plant frags, sparce rhizodont scales, sparce ostracods
343.45	grey	mudstone clasts, soft sed def	abundant plant frags, megaspores, bone frags, cuticle
345.5	grey/red	grades into red silt at top	plant and bone frags, rhizodont scales
348.55	grey	soft sed deformation, clay rip-ups	abundant plant frags, charcoal, fish scales, actinopt and rhizodont frags
353.4	grey	silt clasts	rooted, plant frags, common actinopt and rhizodont frags, sparce ostracods
360.9	grey	disrupted structure	plant, actinopt and cuticle frags
361.55	grey	cm thick beds, red and black silt clasts	plant and fish scale frags
364.05	green/grey	laminated, organic-rich	plant frags, bone frags?
365.35	grey	1cm thick black mudstone bed within silt	plant frags, rhizodont and actinopt scales, bone frags
366.85	grey	green mottles, disrupted laminae	fish scale frag, lungfish bone frag?
368.75	grey	disrupted laminae, slickensides	fish scale frag, plant frags
372.55	grey	clay-rich, common slickensides	fish frags, shell frags, ostracod?
374	black	bedded, organic-rich, soft sed def	abundant plant frags, tetrapod, shrimp, fish bone and cuticle frags
377.2	grey	soft sed def, slickensides, grey and red silt clasts	plant, fish scale and cuticle frags
379.45	grey	organic-rich, slickensides, brecciated, pedogenic	rooted
388.1	red	pedogenic, mottled, brecciated, slickensides	rooted, plant and fish scale frags

391.38	red	pedogenic, slickensides	rooted
417.65	grey/green	no laminae, clasts of red silt	plant frags, small bone frag, actinopt scales
418.05	red	pedogenic, mottled, slickensides	roots?
421.3	grey	massive, slickensides, sparce clasts	plant frags, indet. shelly fossil frags
472.9	grey/green	grey/red/green, cracks	plant frags
473.95	red	red/yellow mottles, brecciated, pedogenic	plant, cuticle, actinopt and rhizodont frags
474.87	black	black and red silt clasts, brecciated, pedogenic	
476.8	green	fine green silt matrix , rip-ups	plant frags, fish scales, ostracods
477.4	green	green silt matrix, rip-ups	fish, plant and shell frags
489.8	grey	clasts of mud and coarse silt, laminated	large plant frags, biot top, ostracods (poor), actinopt frags
490.4	grey	sparce black mud clasts	plant frags
490.95	grey	laminated, water escape, soft sed def, small clasts	biot, plant frags, ostracods (poor), rhizodont scales
491.35	grey	laminated, sandy laminae, small clasts, silt-rich	*Serpula* sp.
508.37	grey	clasts of silt and sand	biot

Appendix 1. Key features of sandy siltstone beds present in the Norham Core and Burnmouth field section. Beds are listed in stratigraphic order, with information on the bed thickness, colour, lithological features and fossil content. The thickness of beds from Burnmouth is not included due to the high level of error derived limits to bed exposure in the field. Height is given from the position of the centre of the sandy siltstone bed. Thin sections of the following beds were measured for clast composition and clast size: Burnmouth: 180.9 m, 334.85 m, 338.35 m, 340.55 m and 477.4 m; Norham Core: 442.74 m, 381.91 m, 218.67 m, 156.58 m and 156.45 m. Abbreviations: actinopt = actinopterygian, biot = bioturbation, frags = fragments, silt = siltstone, soft sed def = soft sediment deformation.

Facies association	Facies	%	Facies description	Depositional environment
Fluvial	Cross-bedded sandstone	20.1	Metre-thick cross-bedded fine-medium sand with grey silt rip-up clasts. Erosive surfaces and lateral accretion indicate stacking of multiple channels. Stacked units ≤23 m thickness in Core and ≤36 m in field section	Meandering to anastomosing fluvial channels
	Rippled sandstone–siltstone	12.3	Silt or fine sand, with trough cross to climbing ripple lamination, occurs above the cross-bedded sandstone facies. Bed thickness in Core 1 to 265 cm, mean 29 cm. Successions grade into laminated grey siltstone, tops commonly rooted	Mid to top of fluvial channel
	Conglomerate lag	0.4	Laterally discontinuous units 0.05 to 1 m thick in field section. Sandstone matrix, Pebble-sized clasts composed of siltstone, cementstone and bioclasts. Erosive base, matrix-supported, grades into the cross-bedded sandstone facies	Base of fluvial channel
Overbank	Laminated grey siltstone	15.8	Laminated grey siltstone without desiccation cracks or pedogenic modification. Commonly interbedded with sand laminae or centimetre-thick beds. Plant fossils and bioturbation common	Floodplain lakes
	Sandstone	13.8	Lenticular or thinly-bedded units that occur in between siltstones and palaeosols. Grain size very fine to fine, cross-bedded to planar or cross-laminated. Beds grade into laminated grey siltstone, rooted horizons common	Overbank flooding into temporary floodplain lakes and small stream deposits
	Palaeosol	15.0	Rooted siltstones–mudstones lacking primary sedimentary structures. Thickness 0.02 to 1.85 m in core, units are grey (51%) or red (48%). Roots preserved as carbonised films or drab root haloes, 1 to 80 cm root depth. Siderite nodules and carbonate nodules occasionally present in grey and red palaeosols, respectively. Vertical cracks ≤38cm in length and smaller polygonal cracks common in red palaeosols, commonly filled with sandy siltstone facies	Sub-aerial floodplain, with a diverse vegetation cover
	Sandy siltstone	5.6	Matrix-supported grey to black siltstones with sand-sized rip-up clasts composed of siltstone, palaeosol, very fine sandstone and common bioclasts. Beds <10 cm thick are most common, units fine-upward into laminated grey siltstone	Out of channel, unconfined flow deposit onto floodplain and deposition in temporary lakes

	Lenticular conglomerate	0.0	Conglomerate lenses on average 20 cm thick, occur in between siltstones and palaeosols. Lateral extent of a few metres, matrix to clast-supported. Sandstone matrix 0.5 to 1 cm sized clasts composed of siltstone, cementstone and bioclasts	Out of channel, unconfined flow deposit onto floodplain
Saline – lake	Cementstone	13.9	Flat-lying, ferroan dolomite beds composed of dolo-micrite and dolo-microspar within a clay and silt matrix. Rarer nodular horizons present commonly associated with roots. Bed thickness 1 to 140 cm, mean 20 cm	Brackish floodplain lakes, likely euryhaline hypersaline salinity range
	Evaporite	3.0	Gypsum and anhydrite occurring within massive cementstone or laminated grey siltstone. Bed thickness in Core 3 – 103 cm, mean 37 cm. Morphologies range from nodular to chicken-wire to micro-nodules within silt laminae	Evaporite precipitation in sabhka or hypersaline lakes

Table 1. Facies Analysis of the Ballagan Formation. The facies volume (%) is based on thickness measurements from the 490 m long Norham Core, which contains a more complete (well-preserved) record of fine-grained sediments than the field section. Facies descriptions are based on Norham Core and Burnmouth field section observations.

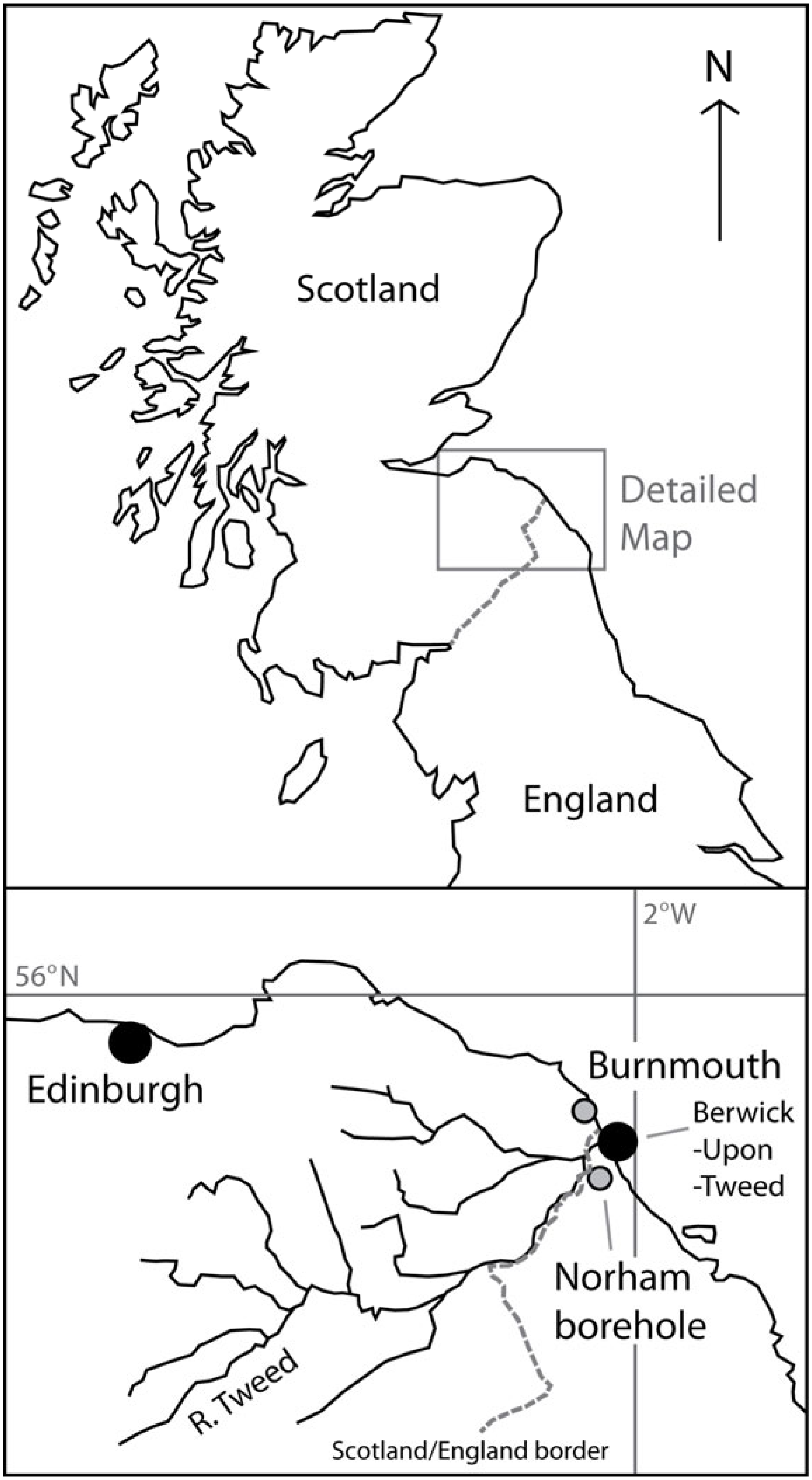
N
Scotland
Detailed
Map
England
2°W
56°N
Edinburgh
Burnmouth
Berwick
-Upon
-Tweed
Norham
borehole
R. Tweed
Scotland/England border

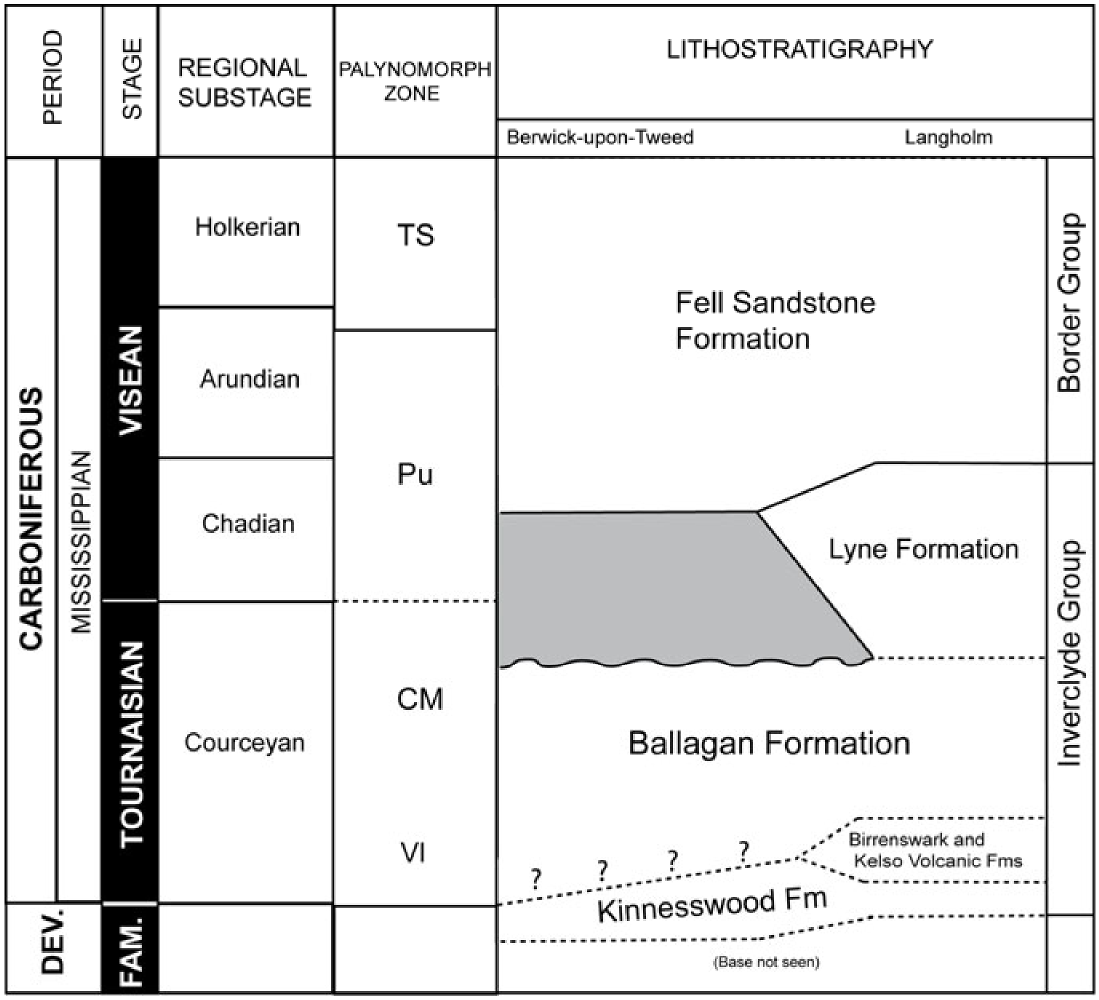
PERIOD
STAGE
REGIONAL SUBSTAGE
PALYNOMORPH ZONE
LITHOSTRATIGRAPHY
Berwick-upon-Tweed
Langholm
CARBONIFEROUS
MISSISSIPPIAN
VISEAN
TOURNAISIAN
DEV.
FAM.
Holkerian
Arundian
Chadian
Courceyan
TS
Pu
CM
VI
Fell Sandstone Formation
Border Group
Lyne Formation
Inverclyde Group
Ballagan Formation
Birrenswark and Kelso Volcanic Fms
Kinnesswood Fm
(Base not seen)

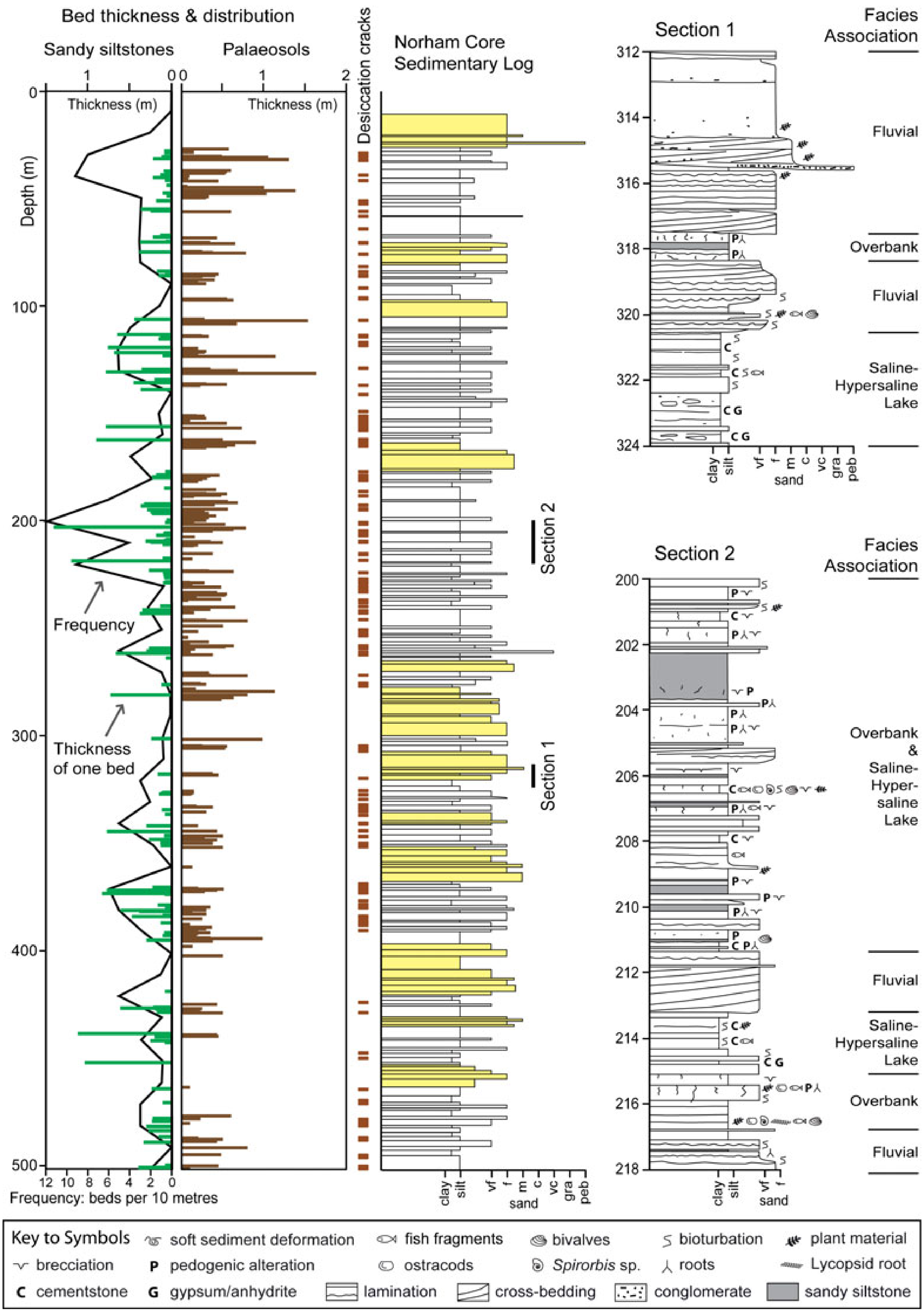

Bed thickness & distribution
Sandy siltstones
Palaeosols
Thickness (m)
Thickness (m)
Depth (m)
Desiccation cracks
Norham Core Sedimentary Log
Frequency
Thickness of one bed
Frequency: beds per 10 metres
Section 1
Section 2
clay
silt
vf
f
m
c
vc
gra
peb
sand
Facies Association
Fluvial
Overbank
Saline-Hypersaline Lake
Overbank & Saline-Hyper-saline Lake
Key to Symbols
soft sediment deformation
fish fragments
bivalves
bioturbation
plant material
brecciation
pedogenic alteration
ostracods
Spirorbis sp.
roots
Lycopsid root
cementstone
gypsum/anhydrite
lamination
cross-bedding
conglomerate
sandy siltstone

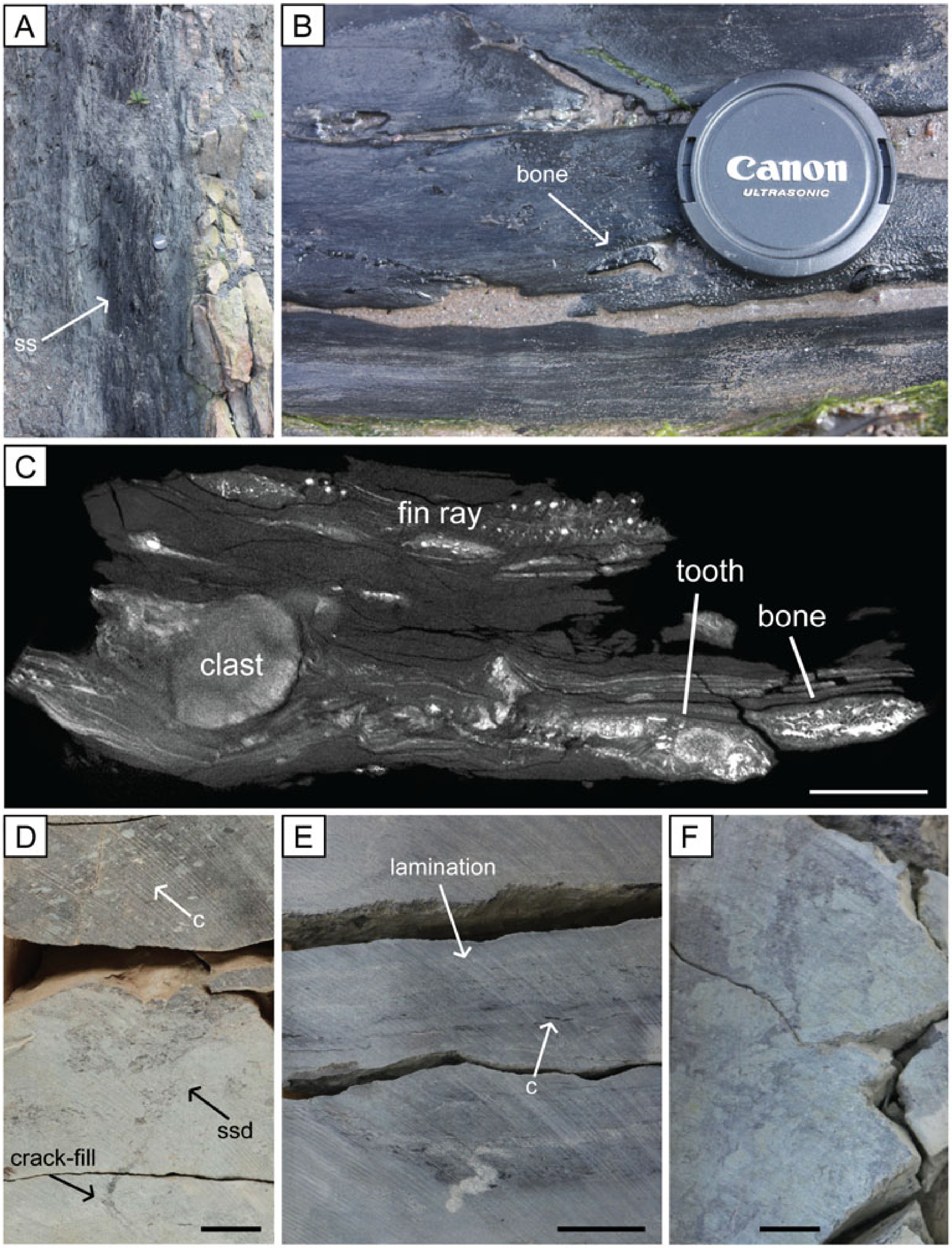
A
ss
B
bone
Canon
ULTRASONIC
C
fin ray
tooth
bone
clast
D
c
ssd
crack-fill
E
lamination
c
F

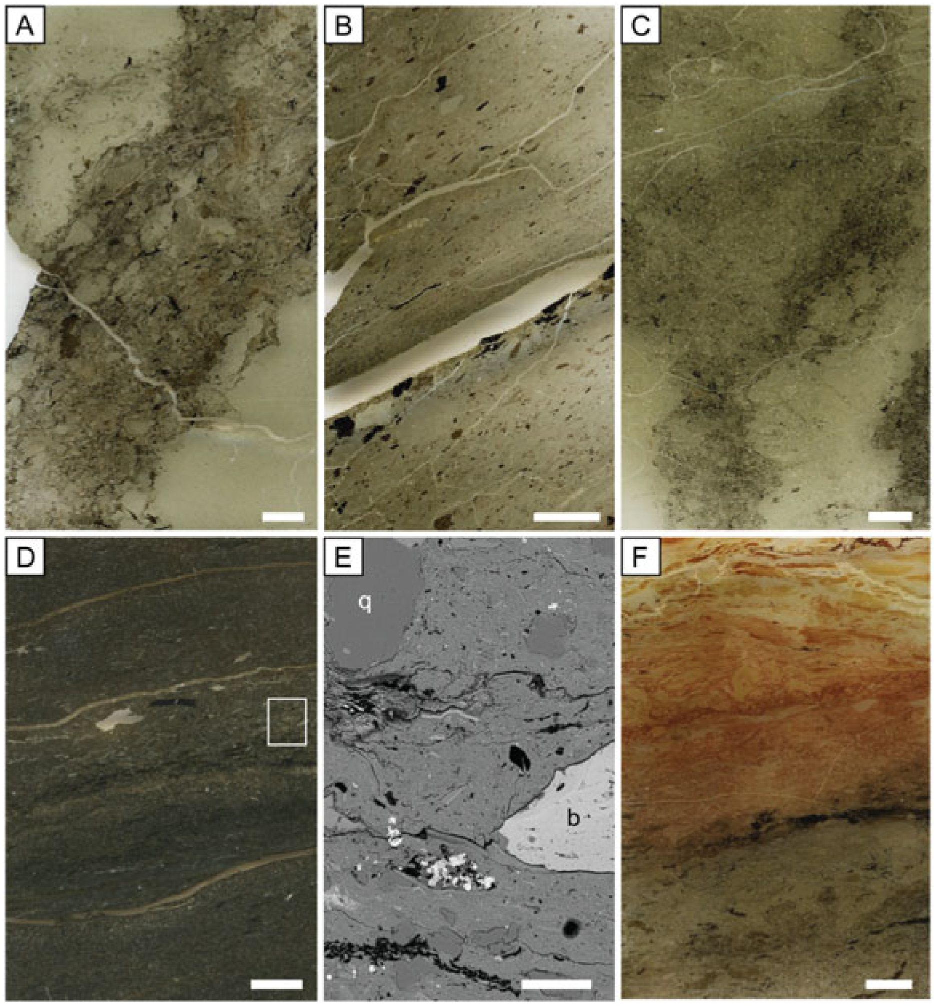
A
B
C
D
E
q
b
F

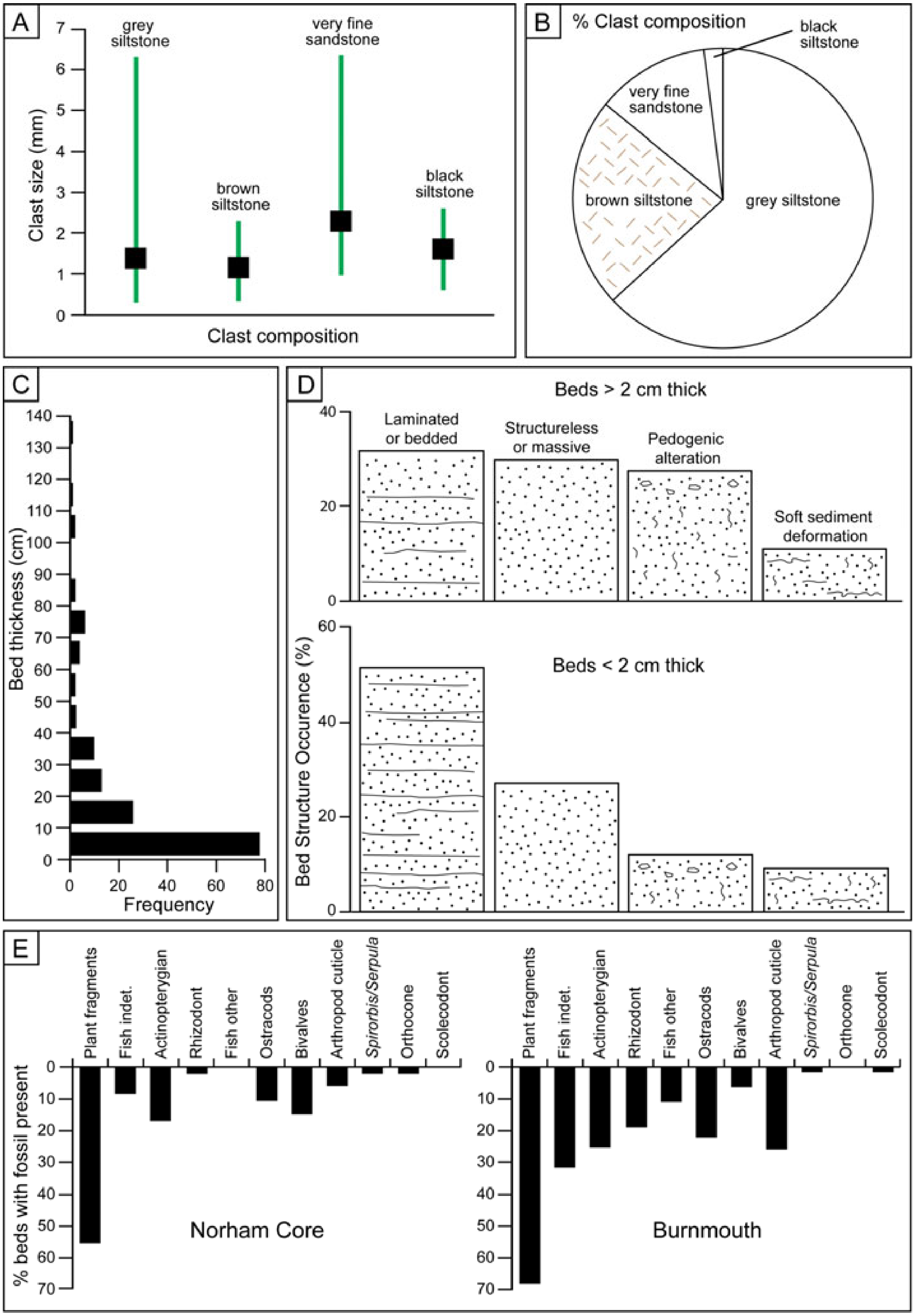
A
grey siltstone
brown siltstone
very fine sandstone
black siltstone
Clast size (mm)
Clast composition
B
% Clast composition
black siltstone
very fine sandstone
brown siltstone
grey siltstone
C
Bed thickness (cm)
Frequency
D
Beds > 2 cm thick
Laminated or bedded
Structureless or massive
Pedogenic alteration
Soft sediment deformation
Beds < 2 cm thick
Bed Structure Occurence (%)
E
Plant fragments
Fish indet.
Actinopterygian
Rhizodont
Fish other
Ostracods
Bivalves
Arthropod cuticle
Spirorbis/Serpula
Orthocone
Scolecodont
% beds with fossil present
Norham Core
Burnmouth

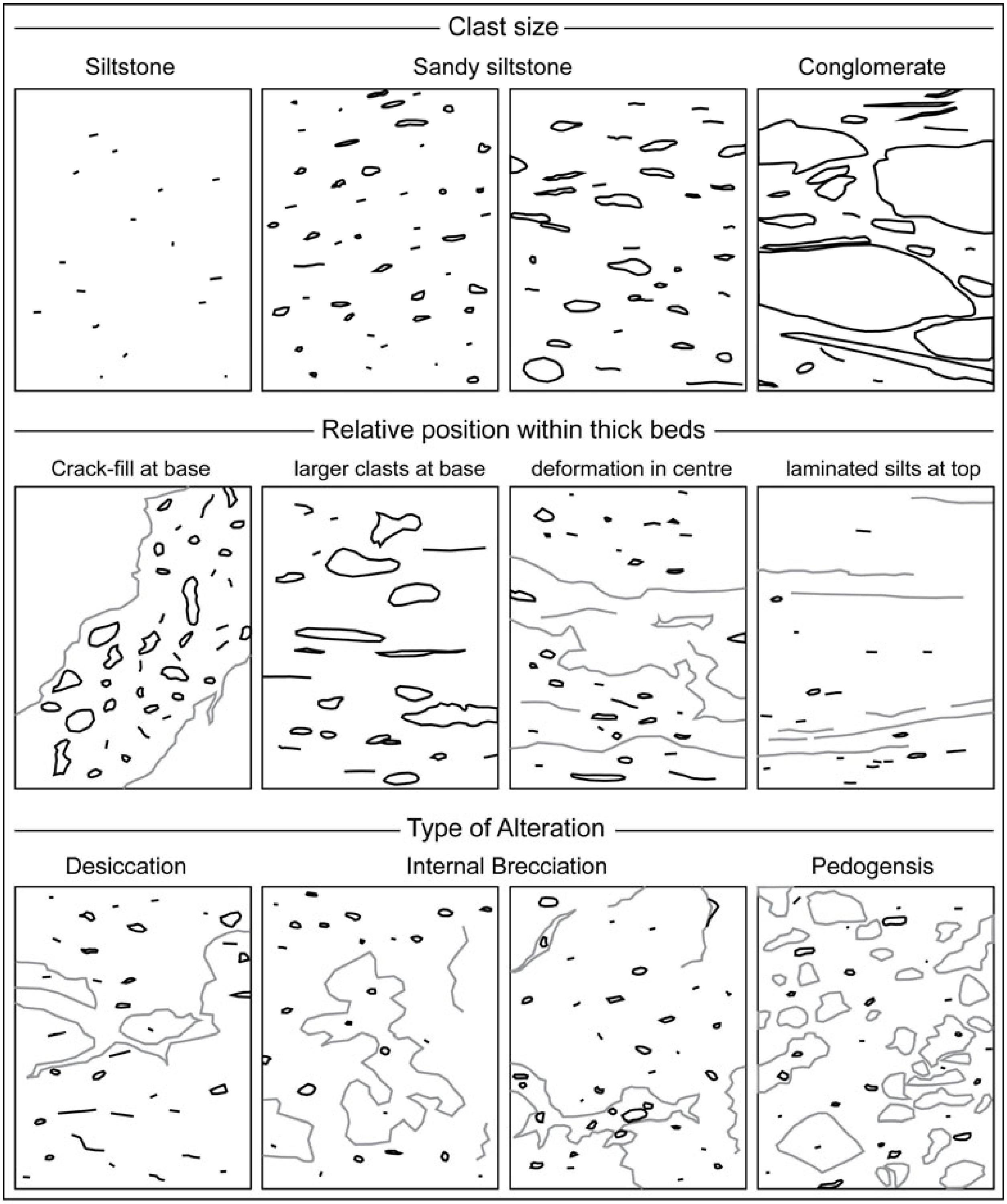
Clast size
Siltstone
Sandy siltstone
Conglomerate
Relative position within thick beds
Crack-fill at base
larger clasts at base
deformation in centre
laminated silts at top
Type of Alteration
Desiccation
Internal Brecciation
Pedogensis

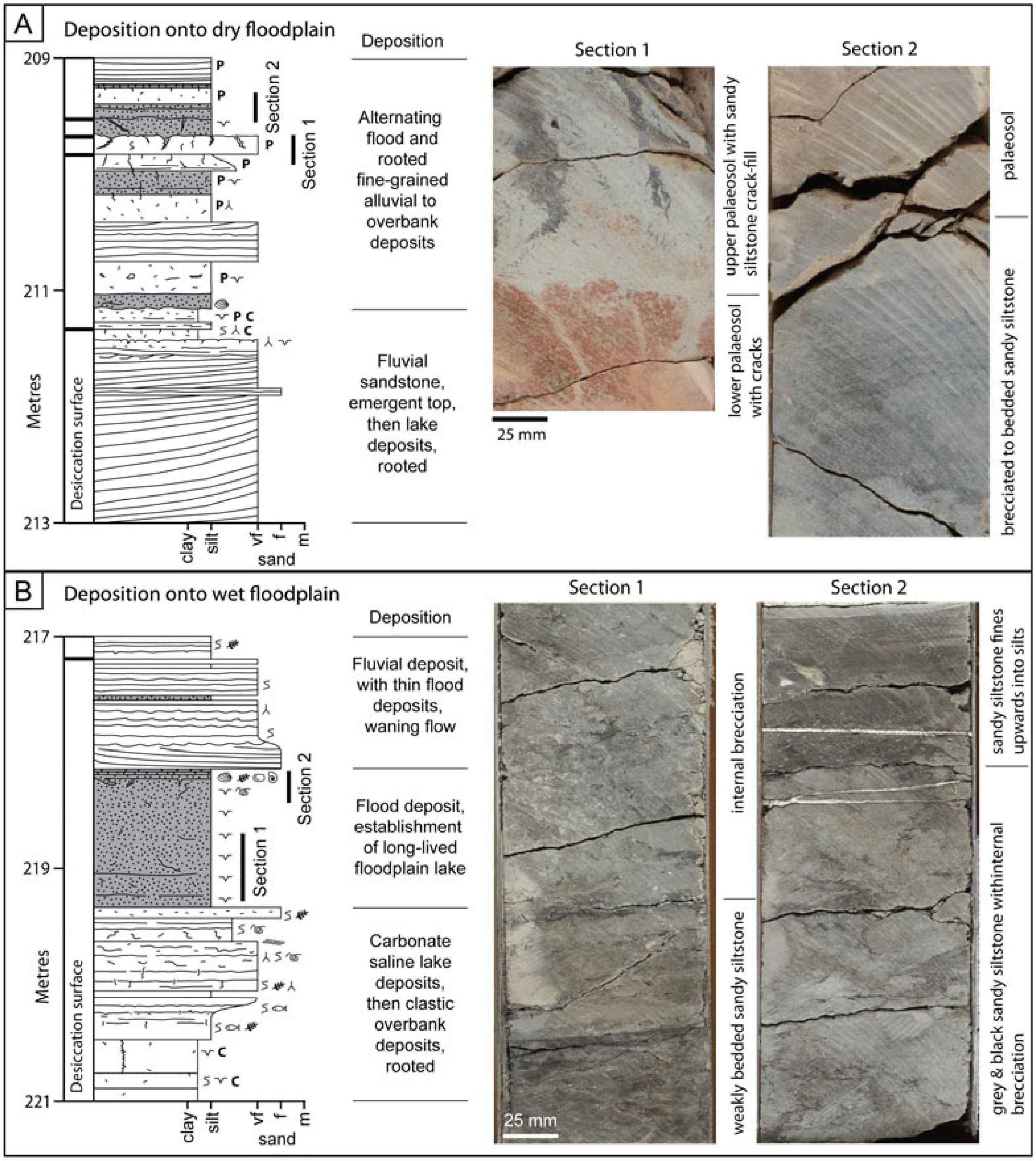
A
Deposition onto dry floodplain
Deposition
Alternating flood and rooted fine-grained alluvial to overbank deposits
Fluvial sandstone, emergent top, then lake deposits, rooted
Section 1
Section 2
upper palaeosol with sandy siltstone crack-fill
lower palaeosol with cracks
palaeosol
brecciated to bedded sandy siltstone
25 mm
209
211
213
Metres
Desiccation surface
clay
silt
vf
f
m
sand
B
Deposition onto wet floodplain
Deposition
Fluvial deposit, with thin flood deposits, waning flow
Flood deposit, establishment of long-lived floodplain lake
Carbonate saline lake deposits, then clastic overbank deposits, rooted
Section 1
Section 2
internal brecciation
weakly bedded sandy siltstone
sandy siltstone fines upwards into silts
grey & black sandy siltstone withinternal brecciation
25 mm
217
219
221
Metres
Desiccation surface
clay
silt
vf
f
m
sand

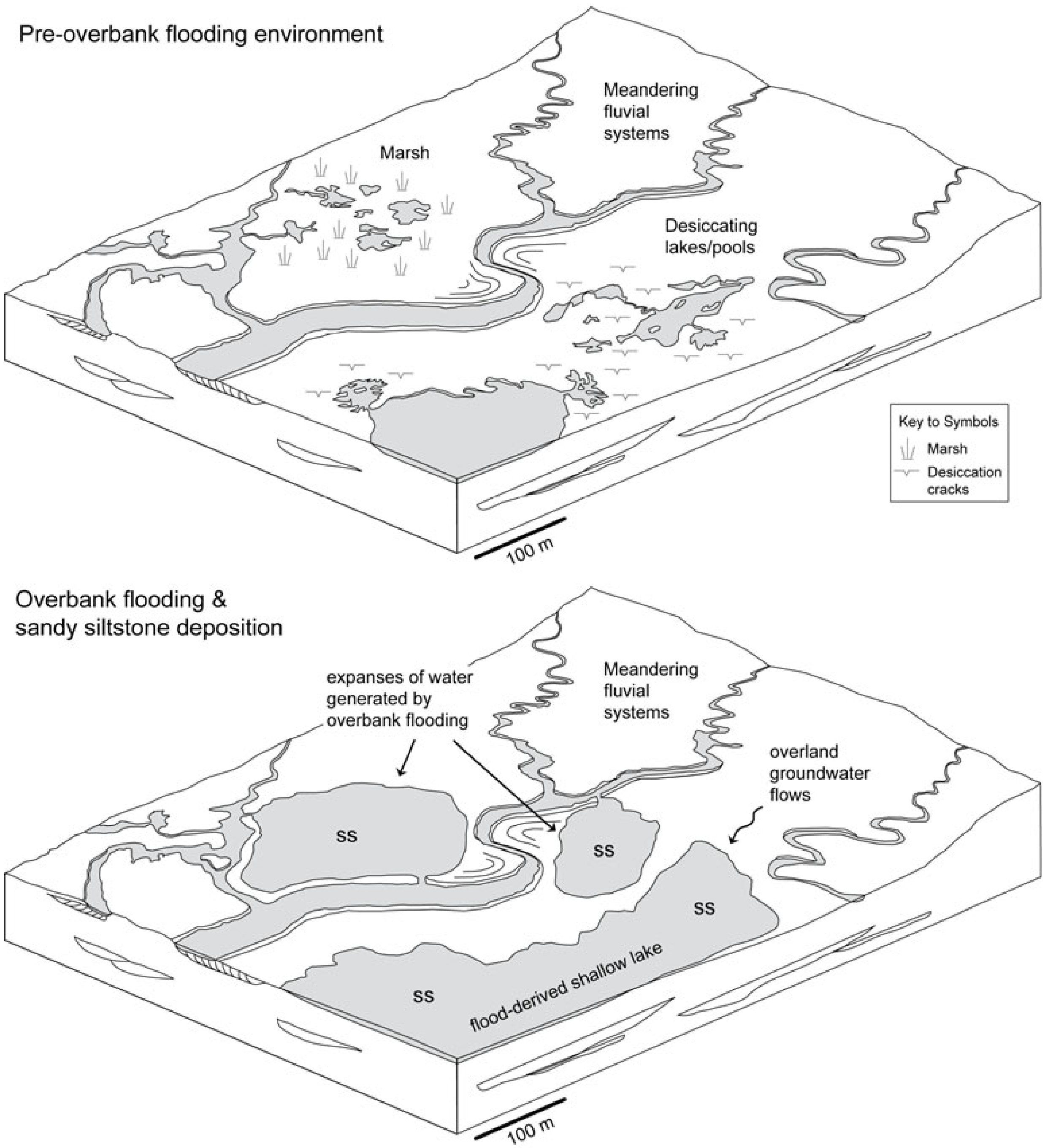
Pre-overbank flooding environment
Meandering fluvial systems
Marsh
Desiccating lakes/pools
Key to Symbols
Marsh
Desiccation cracks
100 m
Overbank flooding & sandy siltstone deposition
expanses of water generated by overbank flooding
Meandering fluvial systems
overland groundwater flows
ss
ss
ss
ss
flood-derived shallow lake
100 m